



Provenance of Late Mesozoic Strata and Tectonic Implications for the Southwestern Ordos Basin, North China: Evidence from Detrital Zircon U-Pb Geochronology and Hf Isotopes

Zuoqiang Li^{1, 2, 3}, Fengjie Li^{*1, 2}, Zheng'an Chen², Xuelian Lai², Xiaokang Ma²

1. State Key Laboratory of Oil and Gas Reservoir Geology and Exploitation, Chengdu University of Technology, Chengdu 610059, China

2. Institute of Sedimentary Geology, Chengdu University of Technology, Chengdu 610059, China

3. 207 Geological Brigade of Sichuan Bureau of Exploration & Development of Geology & Mineral Resources, Leshan 614000, China

 Zuoqiang Li: <https://orcid.org/0000-0001-8631-1261>;  Fengjie Li: <https://orcid.org/0000-0001-8900-4064>

ABSTRACT: In order to determine the provenance and variation characteristics of sandstone-type uranium deposits located in the southwest Ordos Basin, U-Pb geochronology and Hf isotope analyses were conducted on detrital zircons from the Late Mesozoic strata of the SD01 well in the Zhenyuan area. The detrital zircon U-Pb ages of four samples exhibited four main peaks at 250–330, 420–500, 1 720–2 000, and 2 340–2 580 Ma, with a small number of zircons dated at 770–1 100 Ma. The detrital zircon age spectrum and further restriction provided by the *in-situ* Hf isotopic data suggest that the provenance of each stratum was mainly derived from the crystalline basement rock series (Khondalites, intermediate-acidic intrusive rocks, and metamorphic rocks) of the Alxa Block to the northwest and the Yinshan Block to the north, with minor amounts of Caledonian magmatic rocks and Jingning Period rocks from the western part of the northern Qilian orogenic belt to the west and the northern Qinling orogenic belt to the south. The provenance of the sandbody has not changed significantly and is of the Middle Jurassic–Early Cretaceous. The clear variations in the zircon ages of the samples from the Zhiluo and Anding formations were likely influenced by climate change during the Middle–Late Jurassic. The Triassic zircon age (<250 Ma) first appeared in Early Cretaceous strata, suggesting that tectonic activity was relatively strong in the northern Qinling orogenic belt during the Late Jurassic and produced extensive outcrops of Indo–Chinese granite, which were a source of basin sediments.

KEY WORDS: Southwestern Ordos Basin, provenance analysis, Late Mesozoic, detrital zircon U-Pb geochronology, Hf isotopes, geochemistry.

0 INTRODUCTION

Sandstone-type uranium deposits are mainly distributed in the basin-mountain junction of the Mesozoic–Cenozoic basins in northern China, and include a series of deposits in the Bayin Gobi, Songliao, Erlian, and Ordos basins (Xie et al., 2020; Rong et al., 2019; Jin et al., 2018; Akhtar et al., 2017; Hall et al., 2017; Fu et al., 2016; Shen et al., 2014). Extensive exploration of these ore deposits has been conducted in the Ordos Basin, including the discovery of a series of sandstone-type uranium deposits in Mesozoic strata. These areas are located in the basin-mountain junction, and the Zhiluo Formation contains the main ore-bearing strata (Akhtar et al., 2017; Jiao et al., 2015; Wang H et al., 2013; Xue et al., 2010; Yang X Y et al., 2009; Liu et al., 2007). Recently, the SD01 well was drilled by the Tianjin Geological Survey Center in the southwestern part of

the basin. During drilling, an industrially significant uranium orebody was discovered in the aeolian sandstones of the Lower Cretaceous Luohe Formation, greatly expanding the prospects for sandstone-type uranium orebodies in the Ordos Basin (Miao et al., 2020a, b; Qiao et al., 2020; Zhao J F et al., 2020a; Zhu et al., 2019). Previous studies only reported a few small uranium deposits in aeolian sedimentary environments, including Mesozoic aeolian sandstones in Colorado in the United States of America (USA). However, most uranium mineralization has only been observed on a small scale (Sanford, 1982; Isachsen et al., 1955).

Studying sandbody provenance is an important prerequisite for prospecting work regarding sandstone-type uranium deposits. Previous studies have been carried out on the petrology (Chen et al., 2019; Luo, 2017; Zhao et al., 2010; He, 2007), geochemistry (Yu et al., 2020; Luo et al., 2017; Wang et al., 2017; Zhou et al., 2017), and detrital zircon U-Pb geochronology of Jurassic sand along the western and southern margins of the Ordos Basin (Yu et al., 2020; Guo et al., 2018a, b; Lei et al., 2017; Zhou et al., 2017; Guo et al., 2010). The provenance of this area is relatively complex, and related studies of the Middle Jurassic Zhiluo Formation and the overlying strata in

*Corresponding author: lifengjie72@163.com

© China University of Geosciences (Wuhan) and Springer-Verlag GmbH Germany, Part of Springer Nature 2022

Manuscript received November 2, 2020.

Manuscript accepted March 10, 2021.

the southwestern part of the basin are not robust. There are few studies on the provenance of the Lower Cretaceous Luohe Formation (Zhu et al., 2018). The formation of sandstone-type uranium deposits requires a stable input of dissolved uranium from the provenance during the metallogenic period, as well as the contribution of uranium contained within the sand reservoir during the synsedimentary period, which is also an essential source of uranium during the metallogenic process (Bonnetti et al., 2015; Jiao et al., 2015). The Middle Jurassic stratum is the main ore-bearing layer in the basin, while the Lower Cretaceous stratum is the ore-bearing layer in the study area. There is still a lack of understanding regarding the corresponding source changes during the Middle Jurassic–Lower Cretaceous in the study area. Therefore, the determination of the Late Mesozoic stratum source can elucidate the pre-enrichment characteristics of uranium and provide some reference for the recovery of the prototype basin at a later stage.

Zircon is a common heavy mineral in various clastic sedimentary rocks. Because the isotopic system has a high sealing temperature and a strong resistance to weathering, it can comprehensively record source-related tectonic events (Zhang et al., 2001; Cherniak and Watson, 2001; Lee et al., 1997). In particular, breakthroughs in detrital zircon U-Pb dating (i.e., using laser ablation-inductively coupled plasma-mass spectrometry (LA-ICP-MS) and U-Pb dating technology) in the past decade have greatly promoted the development of provenance analyses in the Ordos Basin. Detrital zircon U-Pb dating has been successfully used for basin-mountain coupling analyses, and previous studies have accurately determined the provenance of sedimentary rocks, the uranium source area, and the tectonic background using in situ zircon Lu-Hf isotope analyses (Liu et al., 2021; Geng et al., 2020; Zhao X C et al., 2020; Guo et al., 2018a, b; Zhang X et al., 2018; Zhang Z L et al., 2018; Pereira et al., 2016; Xing et al., 2016; Wang H et al., 2013; Thomas, 2011; Wan et al., 2011; Long et al., 2010; Dickinson et al., 2008; Link et al., 2005). Therefore, in this study, we use LA-ICP-MS *in-situ* U-Pb dating and Hf isotope analyses to perform fine-scale dating and Hf isotopic analyses of detrital zircons from the Late Mesozoic strata in the Zhenyuan area of the southwestern Ordos Basin. By comparing the isotope chronology and the nature of the parent rock in the surrounding area, we determine the source area of the Middle Jurassic–Early Cretaceous strata in the Zhenyuan area. Finally, based on the ages of zircons from the Late Mesozoic strata, we discuss the changes in provenance and regional depositional as well as the tectonic setting.

1 GEOLOGIC SETTING

The Ordos Basin is located in the southwestern North China Craton, covering an area of more than 250 000 km² (Fig. 1). The basin is bound by the Tianshan-Xingmeng fold belt to the north and the Qilian-Qinling fold belt to the south, which is adjacent to the Alxa Block and the western margin corridor transition zone. The Ordos Basin is rich in resources such as coal, oil, natural gas, and uranium ore, and is known as “a basin of multiple energy resources” in China (Lei et al., 2017; Xie et al., 2016; Bao et al., 2014; Li and Li, 2011; Li and Wang, 2007). During the Triassic, the collision between the Yangtze Plate and the North China Craton formed the Dabie-Sulu ultra-

high pressure (UHP) orogenic belt and a continental lake basin in the Ordos region. The Ordos Basin began to form at this time, superimposed on the larger Paleozoic basin. The Ordos Basin is a typical polycyclic cratonic basin (Liu et al., 2006; Liu and Yang, 2000). During the Middle Jurassic to Early Cretaceous, the vertical movement inside the basin was relatively weak, while the basin edge experienced intense tectonic activity and deformation. This strong late deformation promoted the migration of oil/gas and provided a redox mechanism for the formation of large sandstone-type uranium deposits (Yang X Y et al., 2009b; Ritts et al., 2004).

The study area is located in the Tianhuan Depression in the southwestern Ordos Basin, adjacent to the Weibei uplift in the south. The regional tectonic faults are mainly northwest and near north trending, with special structural locations. The Cenozoic strata in this area are well preserved. The Middle Jurassic strata are divided into the Yan'an, Zhiluo, and Anding formations from the bottom to the top, while the upper Jurassic strata contain conglomerate deposits of the Fenfanghe Formation that are in unconformable contact with Early Cretaceous strata. The Early Cretaceous strata are divided into the Yijun, Luohe, Huanhe-Huachi, Luohandong, and Jingchuan formations from the bottom to the top. The lithology and sedimentary facies types are mainly fluvial facies, lacustrine sand and mudstones, aeolian sandstone facies, and alluvial fan conglomerates (Qiao et al., 2020; Zhu et al., 2019; Zhang et al., 2008; Wei et al., 2006). The Middle Jurassic Zhiluo Formation is mainly composed of gray-white fine sandstones and medium-coarse sandstones, with some mudstones and a large amount of carbonized plant debris (Fig. 2a). The formation was dominated by sandy braided-river facies in the early depositional stage, and later by meandering river facies and shore-shallow lake facies (Zhao et al., 2009). The Anding Formation is mainly composed of mudstones, marls, and carbonates, with some purple-red sandstones (Fig. 2b). The grain size is relatively fine, and the entire formation is lacustrine. The rocks in the early depositional stage are mainly gray-green, but then abruptly change to purplish-red, possibly indicating an abrupt change in the paleoclimate (Li et al., 2015). The Luohe Formation is mainly composed of fine-medium grained sandstones that are partially intercalated with sandy conglomerates and silty mudstones. The middle and upper sections are red-brown and yellow-brown, while the lower part is mainly light gray and gray-green (Fig. 2c). The climate was relatively hot and arid during the depositional period, when alluvial-fluvial, aeolian-fluvial, and aeolian facies were deposited. Sandstone particles have a high porosity and are well sorted with a loose structure. The Luohe Formation is an important ore-bearing target in the southwestern Ordos Basin (Qiao et al., 2020). The upper part of the Huanhe-Huachi Formation mainly comprises blue-gray mudstones and siltstones, while the lower part primarily contains reddish brown powdered sand mudstones and siltstones, mixed with a small amount of fine-medium sandstones (Fig. 2d). The entire section consists of fine clastic deposits (coastal, shallow lake, and delta facies) that formed in a warm and humid climate.

2 SAMPLING AND METHODOLOGY

Four sandstone samples were used for detrital zircon dat-

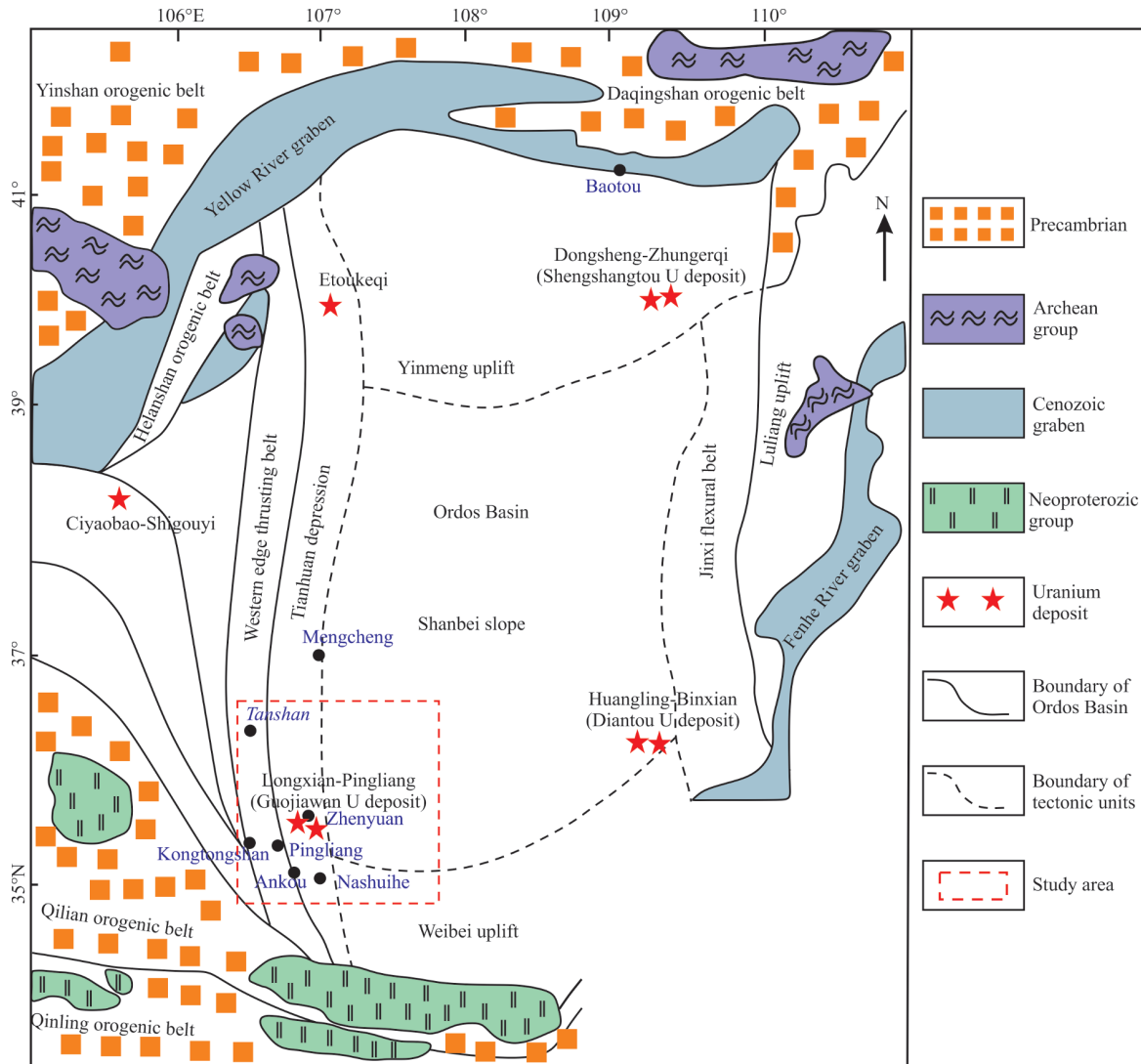


Figure 1. Simplified regional geologic map of the Ordos Basin (modified from Akhtar et al., 2017).

ing in this study. The samples were collected from the 2 000-m-deep SD01 well, which was drilled with the support of the “Northern China Sandstone-type Uranium Deposits Geological Survey” project. The sampling locations in each formation are shown in Fig. 2. The sample collected from the Middle Jurassic Zhiluo Formation (SD01-1) was a gray-white medium-grained sandstone, the sample collected from the Upper Jurassic Anding Formation (SD01-2) was a brick red coarse sandstone, the sample collected from the Lower Cretaceous Luohe Formation (SD01-3) was a gray-white coarse sandstone located near the uranium deposit, and the sample collected from the Lower Cretaceous Huanhe-Huachi Formation (SD01-4) was a pale yellow medium-grained sandstone.

2.1 LA-ICP-MS Zircon Dating

In this study, the zircon targeting, cathodoluminescence image (CL) acquisition, and LA-ICP-MS zircon U-Pb dating and analyses were conducted by the Honest Geological Service Company, Langfang City, Hebei Province. Traditional heavy liquid and magnetic separation methods were used to separate single zircons with a binocular microscope, randomly selecting

more than 300 zircons for analyses. The zircons were fixed on a microscope slide using epoxy resin and then polished. All zircons were imaged using transmitted light, reflected light, and CL (Guan et al., 2002). Zircon U-Pb dating was conducted using an Agilent 7500a ICP-MS (Hewlett Packard, USA). The spot diameter used for the laser ablation was 30 μm , the energy density was 10 J/cm^2 , and the frequency was 10 Hz. The collection times were 10 ms for ^{202}Hg and ^{232}Th , 20 ms for ^{204}Pb and ^{206}Pb , 30 ms for ^{207}Pb , and 15 ms for ^{208}Pb and ^{238}U . For the other elements, the collection time was 6 ms. Three of every 10 samples were analyzed using international standards SRM610, 91500, and GJ-1. The international standard zircon 91500 was used as an external standard. The elemental contents were compared to an external standard (NIST610) to calibrate the concentrations of U, Th, and Pb, and an internal standard element that used ^{29}Si (Yuan et al., 2008). The concentrations of U, Th, and Pb, and the $^{207}\text{Pb}/^{206}\text{Pb}$, $^{206}\text{Pb}/^{238}\text{U}$, $^{207}\text{Pb}/^{235}\text{U}$, and $^{208}\text{Pb}/^{232}\text{Th}$ ratios were calculated using the GLITTER 4.0 program (Macquarie University, Sydney, Australia). The normal Pb correction was carried out according to the methods described by Andersen (2002), and the age calculations and Concordia dia-

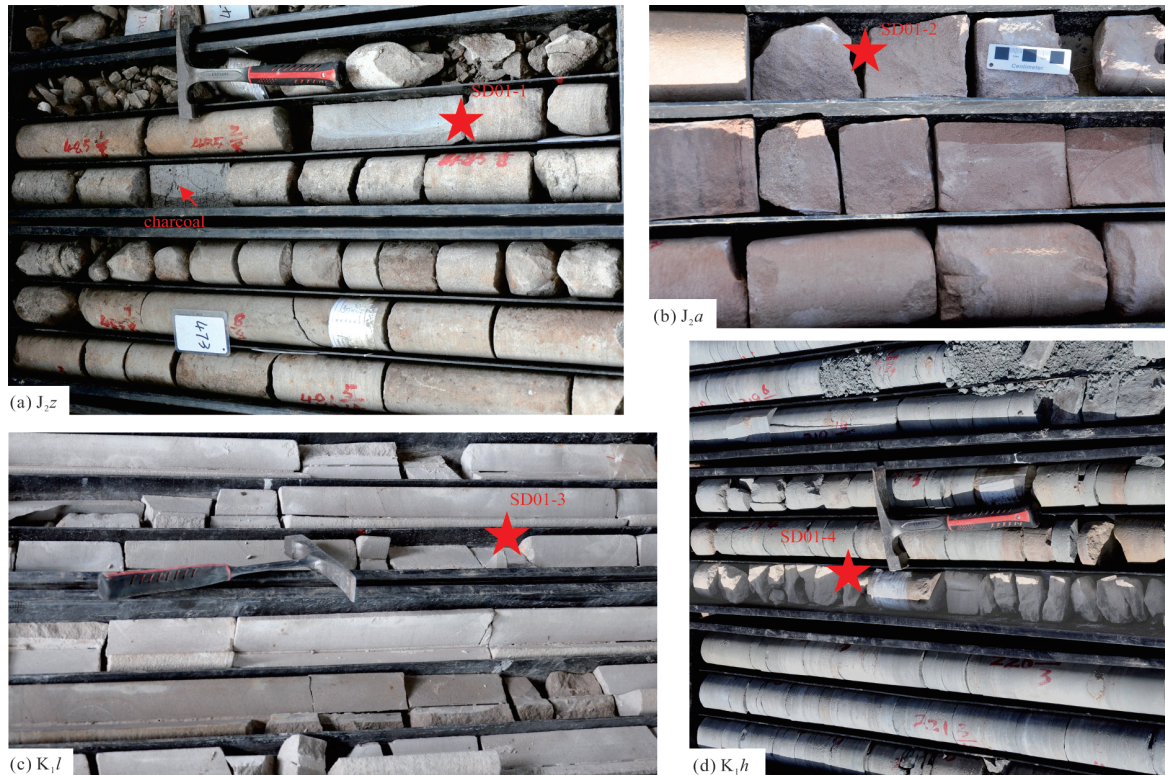


Figure 2. SD01 well core photos of Zhenyuan area, southwest Ordos Basin. (a) Zhiluo Formation, grayish-white medium sandstone, containing a large amount of carbonized plant debris, 1 835–1 840 m; (b) Anding Formation, amaranth medium-coarse sandstone, 1 553–1 556 m; (c) Luohe Formation, light grey coarse sandstone, 1 407–1 412 m; (d) Huanhe-Huachi Formation, pale yellow medium sandstone, 923–931 m. The sample location and sample number are shown in the figure.

grams were generated using the Isoplot 3.75 software package (Ludwig, 2012). The errors (standard deviations) in the isotopic ratios and ages were all determined at the 1σ level. All analytical results are shown in Tabs S1.

2.2 Zircon Lu-Hf Isotopic Analyses

The Lu-Hf isotopic analyses were performed on a Thermo Fisher Neptune Plus multi-collector (MC)-ICP-MS equipped with a 193 nm laser sampling system at the Honest Geological Service Company, Langfang City, Hebei Province. The spot diameter is 44 μm , the ablation frequency was 8 Hz, the energy density is 15–20 J/cm^2 , and the ablation time is 60 s (Xie et al., 2008; Wu et al., 2006). The Lu-Hf isotopic measurements were either made in the same spots or in the same age domains of zircon grains with concordant U-Pb ages (discordance <10%). The operating principles and methods have previously been discussed in detail (Yuan et al., 2008). The zircon Hf isotopic analyses used the international standard zircon 91500 as the isotope correction, and $^{176}\text{Lu}/^{175}\text{Lu}$ and $^{176}\text{Yb}/^{172}\text{Yb}$ ratios of 0.026 69 and 0.588 6, respectively, were used for the interference correction calculations. The $^{176}\text{Lu}/^{177}\text{Hf}$ and $^{176}\text{Hf}/^{177}\text{Hf}$ values and the data for each datapoint contained a 30 s sample signal. A standard sample was analyzed after each set of 10 analyses to monitor instrument drift. The $\epsilon_{\text{Hf}}(t)$ and model age calculation parameters included a decay constant (λ) of 1.867×10^{-11} ; $^{176}\text{Lu}/^{177}\text{Hf}$ and $^{176}\text{Hf}/^{177}\text{Hf}$ ratios of 0.033 2 and 0.282 772, respectively, for chondrite, and 0.038 4 and 0.283 25, respectively, for the depleted mantle; and $f_{\text{Lu/Hf}}$ values of -0.72 and 0.6 for

the upper crust and depleted mantle, respectively (Söderlund et al., 2004; Griffin et al., 2000; Amelin et al., 1999; Blichert-Toft and Albarede, 1997). The formulas used to calculate the $\epsilon_{\text{Hf}}(t)$, T_{DM1} , T_{DM2} , and $f_{\text{Lu/Hf}}$ values of the samples are reported in Wu et al. (2007). All analytical results are shown in Table S2.

3 RESULTS

3.1 Textures of Zircon

Most of the detrital zircons from the 4 samples are light brown and brownish red, although some are colorless. The grain sizes of the zircons are all >100 μm . The CL images showed large variations in their internal structures (Fig. 3); some had nucleus-edge structures, while others have uniform cores. Most of the zircons are round, reflecting their history of weathering and transport over a certain distance. A small number of zircons are columnar and retained a high degree of auto-genesis, suggesting that they were transported from nearby sources. Older zircons tend to be rounder. Most of the zircons developed oscillating or clintheriform zones, which indicate a magmatic origin (SD01-1-45, SD01-2-14, SD01-3-63, and SD01-4-37). However, some zircons had recrystallized, with a number of magmatic zircons containing cores that were inherited or captured (SD01-1-9, SD01-2-52, SD01-3-35, and SD01-4-8). Some of them are typical metamorphic zircons with a homogeneous interior and semi-self-shaped morphology (SD01-3-2 and SD01-3-28). Some of the zircons are metamorphic with edge structures that differed significantly from the core structure (SD01-1-5, SD01-2-29, SD01-3-12, 15, and SD01-4-1, 39).

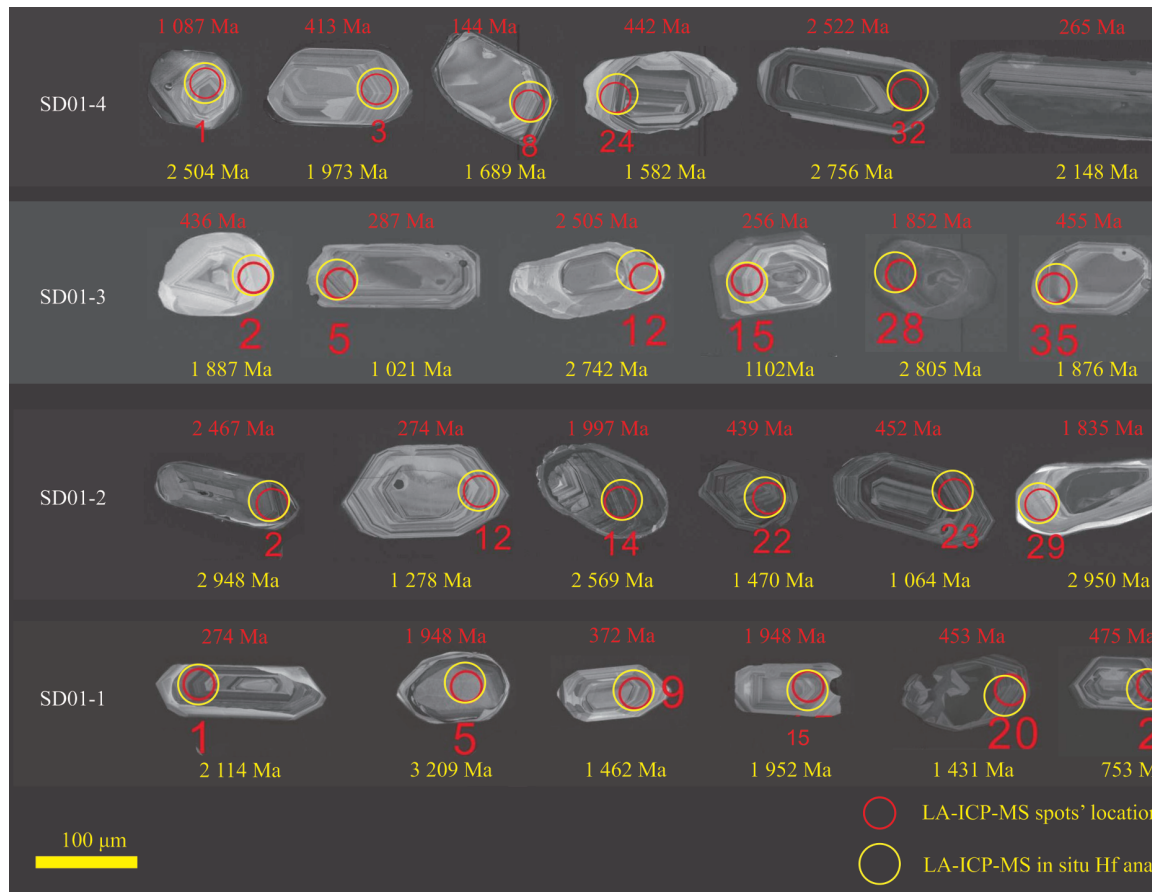


Figure 3. Representative cathodoluminescence (CL) images of the zircons.

The Th and U contents and Th/U ratio are important parameters for determining the source of zircons. Zircons with a Th/U ratio of >0.4 are typically magmatic in origin, while those with a Th/U ratio of <0.1 are typically metamorphic in origin (Wu and Zheng, 2004; Hoskin and Schaltegger, 2003). In this study, most zircons had well-defined oscillating light–dark bands and structures with high U and Th contents (see Table S1). The majority of zircons also had a Th/U ratio of >0.4 and were, therefore, of a magmatic origin (Fig. 4). Some zircons had a Th/U ratio of between 0.1 and 0.4, which may reflect different degrees of metamorphic recrystallization or alteration by later geological events. Only four zircons had a Th/U ratio of <0.1 , thus indicating a metamorphic origin.

3.2 Zircon U–Pb Chronology

A total of 280 data points from the clastic zircons were analyzed. For the young zircons ($<1\ 000$ Ma) that had lower accumulations of radiogenic components, the $^{206}\text{Pb}/^{238}\text{U}$ ages were used to represent the age of zircon formation, while the $^{207}\text{Pb}/^{206}\text{Pb}$ ages were used for the old zircons ($>1\ 000$ Ma) (Blank et al., 2003). Zircon U–Pb ages that met the harmonization requirements (90%–110%) were selected from the data points. Four samples had harmonized ages of 67, 68, 65, and 67, with ages that were generally concordant (Fig. 5). The U–Pb age patterns of detrital zircons from the four samples ranged widely, and the age distribution was summarized as follows (Fig. 6).

Sample SD01-1 was sandstone of the Zhiluo Formation (Middle Jurassic), and showed three major age populations at 250–330, 420–500, and 1 720–2 000 Ma (Fig. 6), accounting for 34%, 15%, and 25% of the total population, respectively. Weak peak age ranges were also observed at 770–1 100 Ma and 2 340–2 580 Ma, accounting for 7% and 7% of the total population, respectively.

Sample SD01-2 was sandstone of the Anding Formation (Middle Jurassic), and presented four major age populations at 270–350, 420–500, 1 730–2 000, and 2 340–2 540 Ma (Fig. 6), accounting for 18%, 21%, 35%, and 13% of the total population, respectively. One zircon was dated at 660 Ma, three zircons were dated at 910–1 135 Ma, and one zircon was dated at 2 972 Ma (i.e., Archean).

Sample SD01-3 was sandstone of the Luohe Formation (Early Cretaceous), and exhibited four major age populations at 220–330, 410–455, 1 720–2 050, and 2 380–2 550 Ma (Fig. 6), accounting for 27%, 23%, 27%, and 16% of the total population, respectively. Two detrital zircons were dated at 1 051 and 1 145 Ma.

Sample SD01-4 was sandstone of the Huanchi-Huahe Formation (Early Cretaceous), and showed four major age populations at 235–330, 390–455, 1 700–1 980, and 2 370–2 540 Ma (Fig. 6), accounting for 36%, 19%, 22%, and 13% of the total population, respectively. Three zircons were dated at 890–1 100 Ma, and one zircon was dated at 144 Ma (i.e., Early Cretaceous).

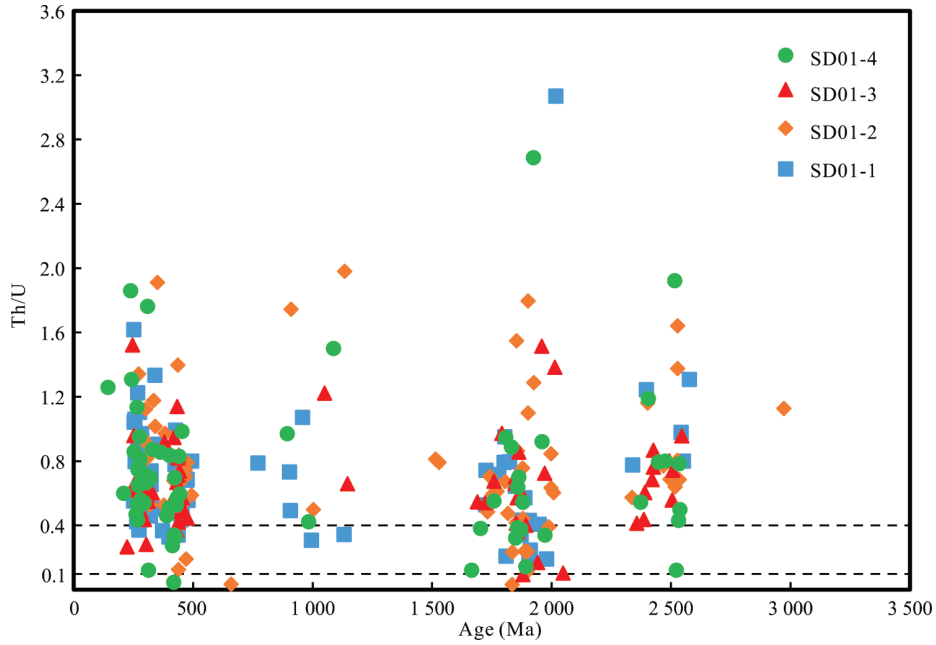


Figure 4. U-Pb age vs. Th/U ratio diagram.

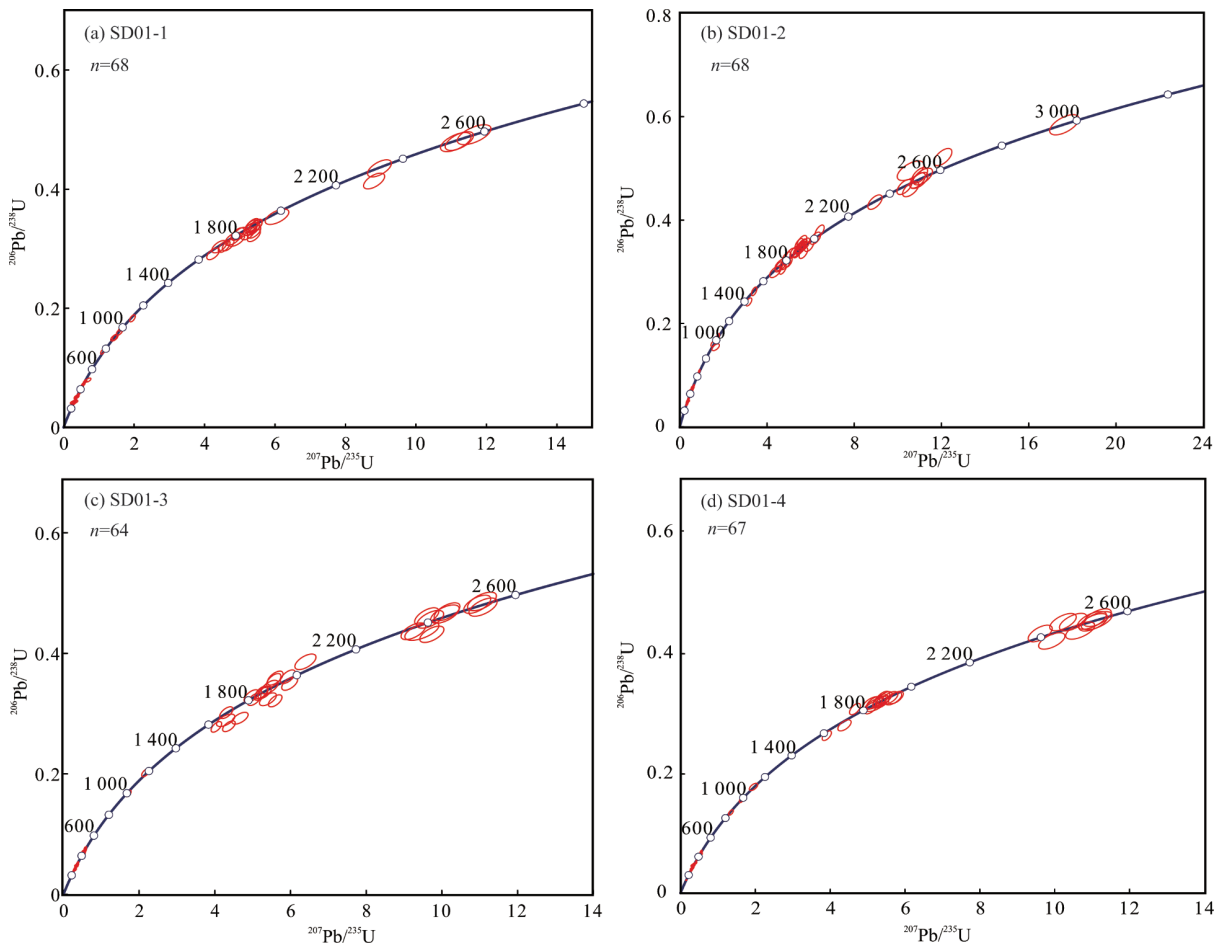


Figure 5. U-Pb concordia diagrams detrital zircons.

3.3 Zircon Hf Isotopes

The zircon $^{176}\text{Lu}/^{177}\text{Hf}$ ratio can indicate the original $^{176}\text{Lu}/^{177}\text{Hf}$ ratio at the time of its formation. Some zircons with

high concordance were selected from each sample for *in-situ* microregional Hf isotopic analyses. The *in-situ* Lu-Hf isotopic compositions of 26 zircons from Sample SD01-1, 25 zircons

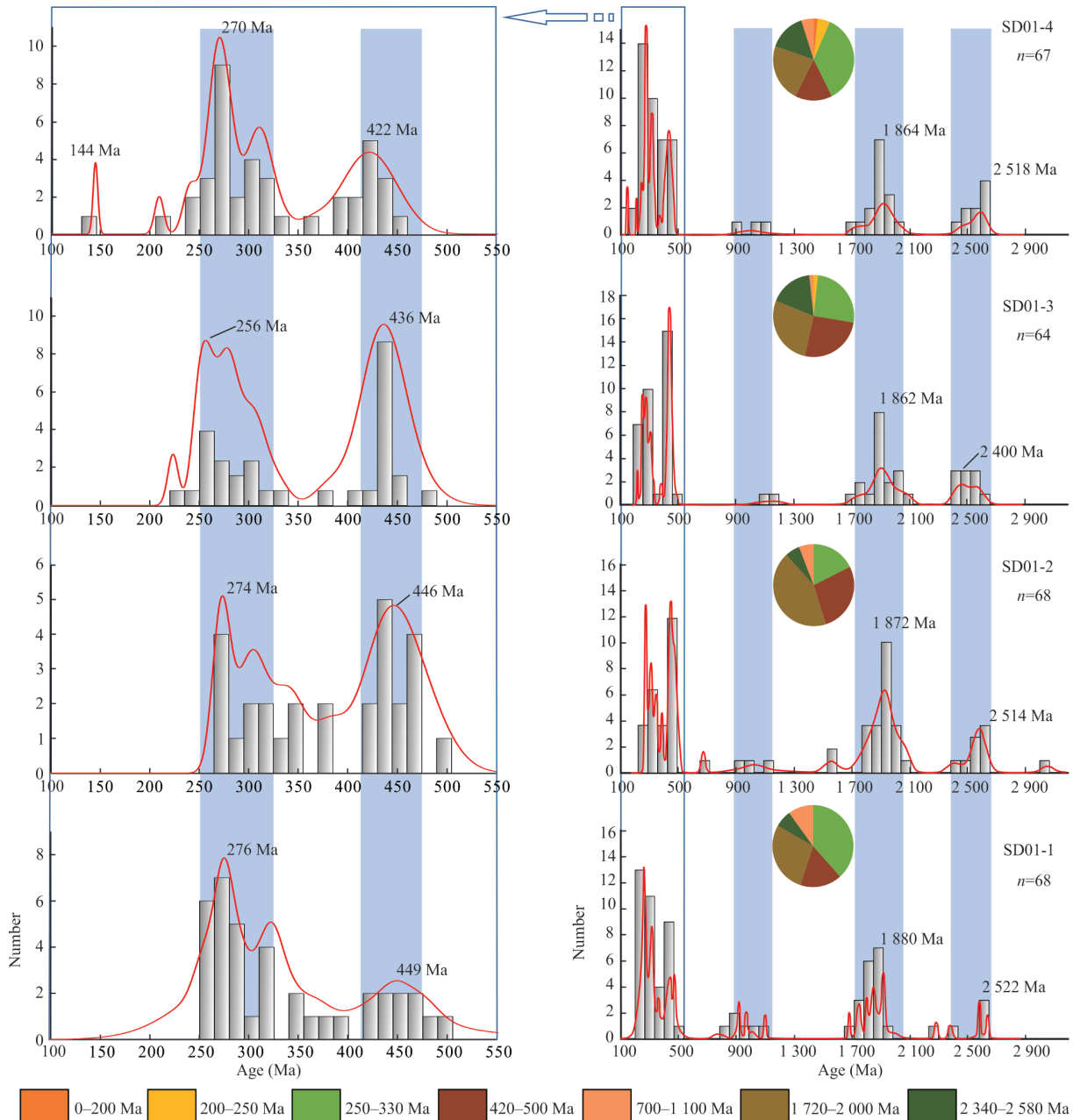


Figure 6. Detrital zircon probability plots.

from Sample SD01-2, 25 zircons from Sample SD01-3, and 25 zircons from Sample SD01-4 were measured. After excluding data with poor Hf isotope signals, all but two zircons had $^{176}\text{Lu}/^{177}\text{Hf}$ ratios of >0.002 , indicating that a very small amount of radioactive Hf accumulated after zircon formation (Kinny and Mass, 2003). Although the $\epsilon_{\text{Hf}}(t)$ values of zircons varied widely from -20.2 to 11.3, most were concentrated between -14 and 7 (Fig. 7), and very few $\epsilon_{\text{Hf}}(t)$ values plotted above the deficit mantle evolutionary line, suggesting that most of the zircons were derived from recycled crustal material. Therefore, the crustal generation ages could be estimated using the two-stage model age (T_{DM2}) (Yang et al., 2009a). The $\epsilon_{\text{Hf}}(t)$ values indicate that the formation of old zircons (>2.0 Ga) was closely related to crustal re-melting, while the formation of new zircons was related to the addition of more mantle material to the

source region since 2.0 Ga. The T_{DM2} ages also ranged widely from 0.7 to 3.2 Ga.

Overall, the Hf isotopic distributions of the four samples were consistent (Fig. 7). The $\epsilon_{\text{Hf}}(t)$ values of the Late Paleozoic zircons were evenly distributed, ranging from -13.5 to 9.9 (average of -1.1), while the T_{DM2} ages ranged widely from 0.7 to 2.2 Ga (average of 1.4 Ga). The $\epsilon_{\text{Hf}}(t)$ values of the Early Paleozoic zircons ranged from -20.2 to 6.0 (average of -6, with most values <0), while the corresponding T_{DM2} ages were between 1.1 and 2.7 Ga (average of 1.8 Ga, with most ages at 1.5–1.9 Ga). Among the seven zircons from the Late Mesoproterozoic to the Early Neoproterozoic, the $\epsilon_{\text{Hf}}(t)$ values of two zircons were -9.1 and -9.2, the $\epsilon_{\text{Hf}}(t)$ value of one zircon was -1.2, and the $\epsilon_{\text{Hf}}(t)$ values of the other four zircons were >0 , with the T_{DM2} ages ranging from 1.5 to 2.5 Ga. The $\epsilon_{\text{Hf}}(t)$ values of the Late

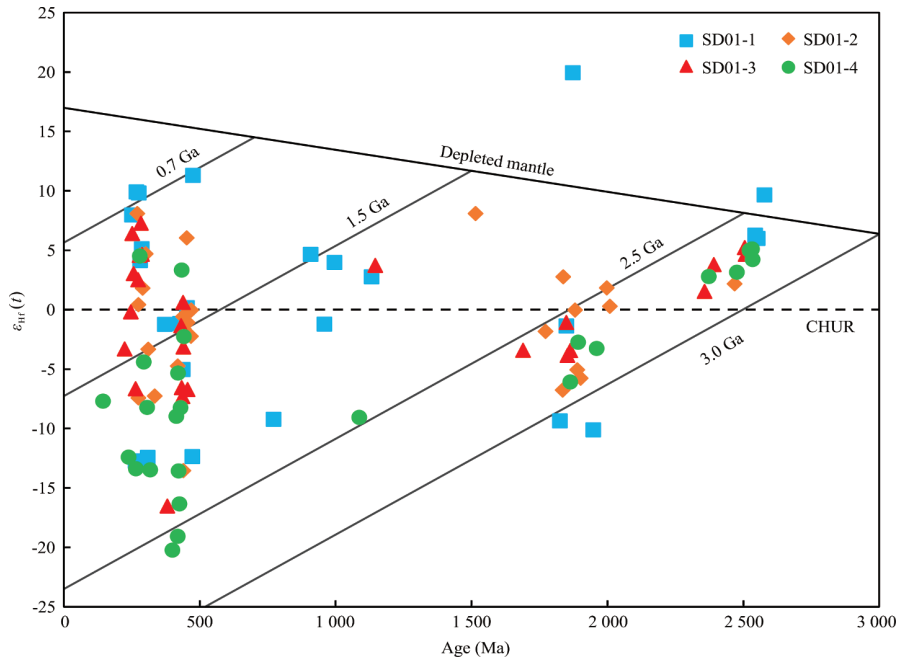


Figure 7. Plot of $\epsilon_{\text{Hf}}(t)$ vs. age (Ma) for the detrital zircons.

Paleoproterozoic zircons ranged from -10.1 to 8.1, with most values < 0; however, one zircon had a value of 20.0, which plotted on the mantle-deficit evolution line. The corresponding T_{DM2} ages were between 1.8 and 3.2 Ga (average of 2.66 Ga, with most ages at 2.6–3.0 Ga). The $\epsilon_{\text{Hf}}(t)$ values of the Early Paleoproterozoic zircons ranged from 1.5 to 9.7 (average of 4.6), and the T_{DM2} ages were between 2.5 and 3.0 Ga (average of 2.8 Ga, with most values at 2.7–2.8 Ga), which were slightly older than the zircon U-Pb ages.

4 DISCUSSION

4.1 Potential Sediment Sources

Extensive sediment source analyses have been conducted along the southern and western margins of the Ordos Basin. Previous studies found that the age distribution of detrital zircons from the Zhiluo Formation was mainly at 220–320, 400–500, 1 600–2 000, and 2 300–2 650 Ma (Yu et al., 2020; Zhao H L et al., 2020; Chen et al., 2019; Guo et al., 2018a, b; Wang et al., 2018; Lei et al., 2017; Luo, 2017; Zhou et al., 2017; Guo et al., 2010; Zhao et al., 2010; He, 2007); hence, the results of the four samples in the present study are consistent with these findings. This agreement suggests that the final provenance could be the same, with only the percentage contribution of each component differing between study areas. The adjacent northern Qilian orogenic belt to the west, the Alxa Block to the northwest, the Yinshan Block along the northern margin of the North China Craton, and the North Qinling orogenic belt to the south may have provided the provenance for the study area. In addition, older sedimentary and metamorphic stratigraphic units may have been the source for the new strata during sedimentation due to tectonic uplift (Zhou et al., 2017). Previous studies on the zircon U-Pb chronology of magmatic and metamorphic rocks in adjacent areas reported a large number of ages. In addition, extensive studies have been conducted on zircon Hf isotope data, which have provided good constraints on

provenance. In order to determine the sediment sources of the four sandstone samples in this study, previously published zircon dating and Hf isotopic data from other areas around the basin were utilized. Combining these data with the findings of the present study can reflect the spatiotemporal distributions of different provenances along the southwestern margin of the Ordos Basin (Figs. 8, 9).

4.1.1 Yinshan Block

The Yinshan Block is located in the northern part of the North China Craton and was formed by typical intra-plate orogenesis (Davis et al., 1998). The Early Precambrian North China Craton underwent multi-stage geologic events and a complex tectonic evolution; continental nuclei and micro-continental blocks formed at >3 Ga, crustal hyperplasia occurred at 2.7–2.9 Ga, the micro-blocks were welded together at 2.5 Ga, and the formation of the North China Craton followed extensive metamorphism and magmatism. The crustal rifting, subduction, and collision processes occurred at 2.3–1.97 Ga, while extension and uplift occurred at 1.97–1.82 Ga. These two groups of events were likely related to the breakup of the Colombian supercontinent. After 1.8 Ga, the entire lower crust was uplifted to form dikes, continental rifts, and non-orogenic magmatism (Meng et al., 2018; Zhai, 2011; Zhai and Santosh, 2011; Rogers and Santosh, 2009; Trap et al., 2007). During the Phanerozoic, the continuous tectonic action in the Central Asian orogenic belt on the North China Craton produced a large Late Paleozoic–Early Mesozoic granite belt in the Yinshan region, with an emplacement age of 235–480 Ma. Currently, granites are widely and extensively exposed in the Yinshan Block (Feng et al., 2020; Zheng et al., 2019; Zhang X et al., 2018; Zhou et al., 2018; Luo et al., 2010, 2007; Zhang et al., 2006).

According to the findings of previous studies, the $\epsilon_{\text{Hf}}(t)$ values of Late Paleozoic magmatism ranged from -16.8 to 5.9 (average of -12.4, with most values < 0), and the corresponding

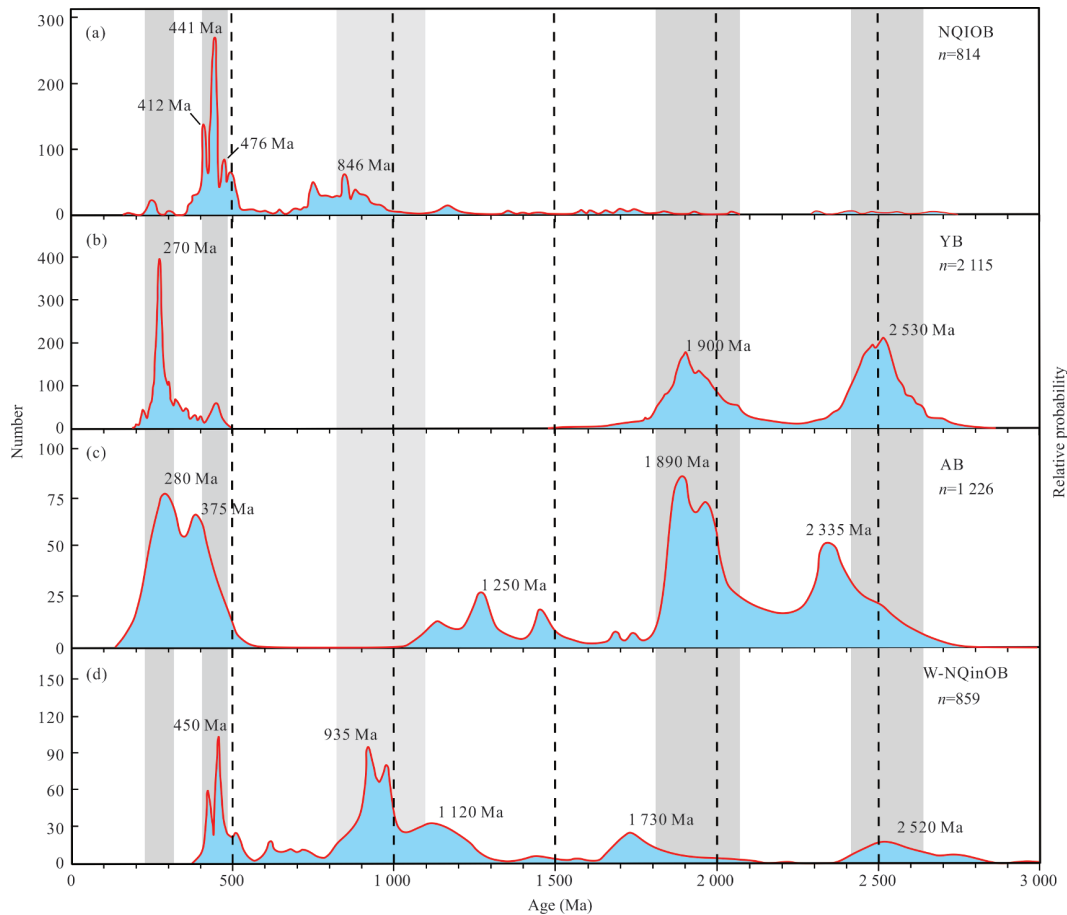


Figure 8. Relative probability density diagram of zircon U-Pb ages for potential source regions. Date sources: (a) the North Qilian Orogenic Belt (NQIOB) are modified from Yang et al. (2015b), (b) the Yinshan Block (YB) are modified from Lei et al. (2017), (c) the Alxa Block (AB), (d) the Western of North Qinling Orogenic Belt (W-NQinOB) are modified from Sun D et al. (2017) and the references therein.

T_{DM2} ages were between 0.9 and 2.4 Ga (average of 1.7 Ga, with most ages at 1.1–2.1 Ga). The $\epsilon_{Hf}(t)$ values of Early Paleozoic magmatism ranged from -6.1 to 6.8 (average of 1.0, with evenly distributed positive and negative values), and the T_{DM2} ages were between 1.0 and 1.8 Ga (average of 1.4 Ga, with most ages at 1.1–1.7 Ga). The $\epsilon_{Hf}(t)$ values of Late Paleoproterozoic magmatism ranged from -7.5 to 4 (average of -0.8, with most values <0), and the T_{DM2} ages were between 2.4 and 3.2 Ga (average of 2.6 Ga, with most ages at 2.4–2.8 Ga). The $\epsilon_{Hf}(t)$ values for the Early Proterozoic ranged from -7.8 to 10.5 (average of 2.8, with most values >0), and the T_{DM2} ages were between 2.3 and 3.9 Ga (average of 2.9 Ga, with most ages at 2.7–3.2 Ga) (Fig. 9).

4.1.2 Alxa Block

The Alxa Block is located on the northwestern margin of the study area and is triangular in shape. The main magmatism in the Alxa Block can be divided into four stages: Early Paleoproterozoic (2 400–2 200 Ma), Middle–Late Paleoproterozoic (2 000–1 810 Ma), Neoproterozoic (1 000–800 Ma), and Phanerozoic (525–175 Ma). Intrusive rocks of all eruption stages are exposed, but the Late Paleozoic granites are the most widely distributed (Guo et al., 2018b; Lei et al., 2017; Dan et al., 2016; Zhang et al., 2012; Zhou and Yu, 1989). The southwestern margin of the Alxa Block was affected by the subduction

and orogenesis of the Qilian Ocean during the Early Paleozoic. The southeastern margin collided with the North China Plate during the Late Paleozoic–Early Mesozoic, and the northern margin was influenced by subduction and accretionary orogeny related to the Paleo-Asian Ocean, which persisted until the Late Paleozoic. Multiple tectonic events are also superimposed in this region and produced massive magmatism (Dan et al., 2016; Zhang et al., 2016; Xiao and Santosh, 2014; Windley et al., 2007; Darby and Gehrels, 2006; Zhang et al., 1997).

Tectonomagmatic events occurred during the Late Paleoproterozoic in the Alxa Block at 2 000–1 900 and 1 850–1 800 Ma, and are mainly exposed in the eastern region (Dan et al., 2012; Geng et al., 2010). Early Neoproterozoic deformable granites form an important part of the basement and are mainly exposed in the western region, with peak ages at 992–978 and 826–807 Ma (Song et al., 2017; Geng and Zhou, 2012; Geng and Zhou, 2010). Recent geochronological studies have shown that a large number of Permian (252–289 Ma) granites are present (Dan et al., 2014; Geng and Zhou, 2012; Shi et al., 2012), which are obvious in the Bayanwula and Langshan areas near the eastern Alxa area (Xie et al., 2020; Zhang J J et al., 2019; Gong et al., 2018; Wang et al., 2016; Wang Z Z et al., 2015; Dan et al., 2014; Geng and Zhou, 2012).

Previous studies found that the $\epsilon_{Hf}(t)$ values of Late Paleozoic magmatism ranged from -23.7 to 7.8 (average of -8.8,

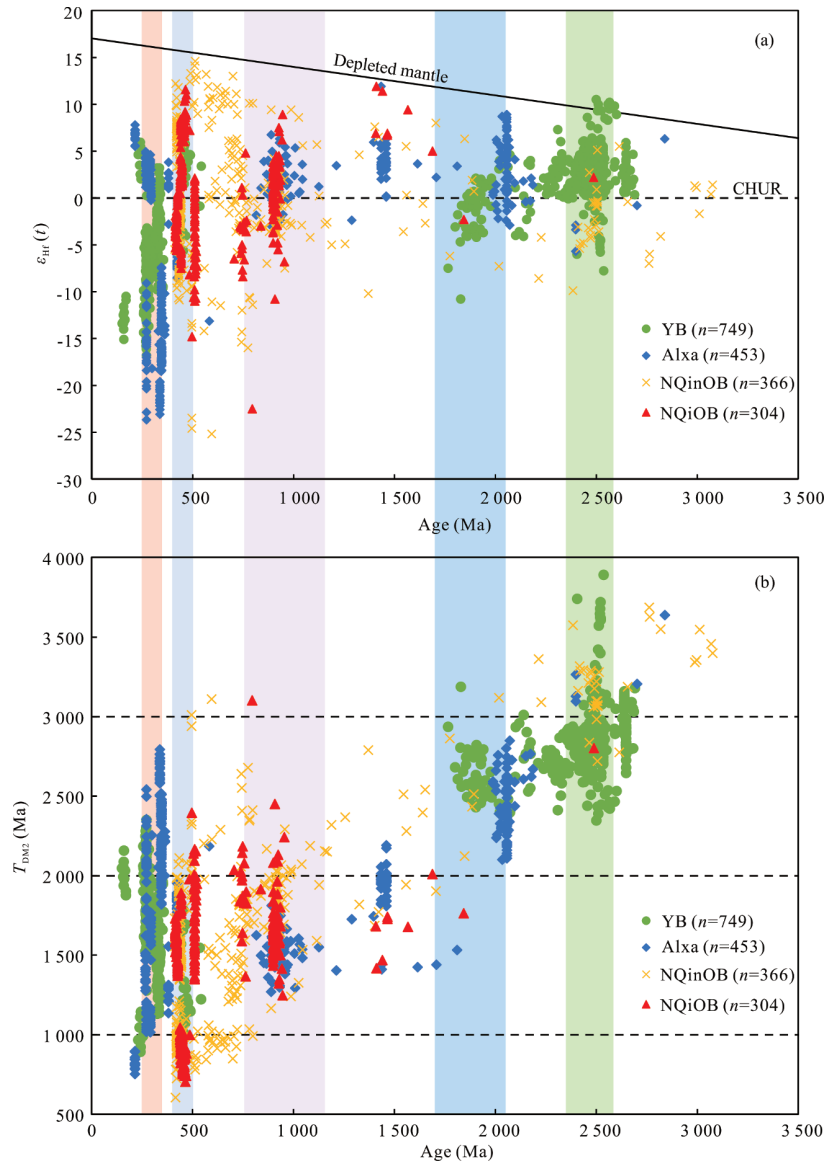


Figure 9. $\epsilon_{\text{Hf}}(t)$ values vs. U-Pb ages (a) and T_{DM2} values vs. U-Pb ages (b). The color bands from left to right correspond to zircon ages respectively: 220–350, 400–500, 770–1150, 1700–2050, 2350–2580 Ma. The Hf isotopic compositions of the Yinshan Block (YB) are collected from Feng et al. (2020), Ouyang et al. (2020), Zheng et al. (2019), Zhang Q et al. (2018), Zhou et al. (2018), Chen et al. (2017), Liu et al. (2016), Su et al. (2014), Bao et al. (2013), Ma et al. (2013, 2011); the Alxa Block (AB) from Shi et al. (2020, 2016), Xie et al. (2020), Zhang J J et al. (2019), Gong et al. (2018), Dan et al. (2016), Geng and Zhou (2012), Geng et al. (2011); the North Qinling Orogenic Belt (NQinOB) are from Qin et al. (2015), Liu et al. (2014), Wang M et al. (2013), Shi et al. (2013), Wang F et al. (2009); the North Qilian Orogenic Belt (NQiOB) from Zhang J Y et al. (2019), Tao et al. (2017), Zhang et al. (2017), Yang et al. (2015), Chen et al. (2014), Yu et al. (2013).

with most values <0), while the corresponding T_{DM2} ages were between 0.8 Ga and 2.8 Ga (average of 1.9 Ga, with ages most at 1.8–2.5 Ga). The $\epsilon_{\text{Hf}}(t)$ values of Meso–Neoproterozoic magmatism ranged from -3.0 to 6.7 (average of 1.8 , with most values >0), and the T_{DM2} ages were between 1.3 Ga and 1.8 Ga (average of 1.5 Ga, with most ages at 1.4 – 1.7 Ga). The $\epsilon_{\text{Hf}}(t)$ values of Late Paleoproterozoic magmatism ranged from -2.9 to 8.9 (average of 3.4 , with most values >0), while the T_{DM2} ages were between 2.1 and 2.8 Ga (average of 2.4 Ga, with most ages at 2.2 – 2.6 Ga) (Fig. 9).

4.1.3 Northern Qilian orogenic belt

The Qilian orogenic belt is located to the west of the

study area. In the Early Paleozoic, the northern Qilian Ocean subducted under the Alxa Block, while the central Qilian Block collided with the Alxa Block to form the Caledonian orogenic belt (Zhao and Jin, 2011; Wu et al., 2010; Xu et al., 2010). The most extensive tectonism recorded in the northern Qilian orogenic belt includes orogenic events during the Early Paleozoic, when a large number of Ordovician–Devonian granite intrusions occurred (400–534 Ma, peak value at ~ 440 Ma). The genesis of these intrusive rocks is associated with deep continental subduction at ~ 500 Ma, crustal thickening caused by continental collision at ~ 450 Ma, and crustal uplift at 420–400 Ma (Qin et al., 2015; Liu et al., 2014; Zhang et al., 2013; Pei et al., 2007b; Yang et al., 2006b). Magmatism also occurred in the

Neoproterozoic, which was related to the convergence and breakup of the Rodinia supercontinent and corresponding island-arc magmatism. These ages can be divided into three stages: 902–981, 839–862, and 738–799 Ma (Gao et al., 2013; Shi et al., 2013; Pei et al., 2012; Wang et al., 2012; Pei et al., 2007a; Lu et al., 2004).

Previous studies reported that the $\epsilon_{\text{Hf}}(t)$ values of Early Paleozoic magmatism ranged from -11 to 11.6 (average of 0.8, with uniformly distributed positive and negative values), while the T_{DM2} ages were between 0.7 and 2.4 Ga (average of 1.3 Ga, with ages concentrated at 0.8–1.0 and 1.3–1.9 Ga). The $\epsilon_{\text{Hf}}(t)$ values of Meso–Neoproterozoic magmatism ranged from -6.8 to 8.9 (average of 0.9, with evenly distributed positive and negative values), and the T_{DM2} ages were between 1.2 and 2.2 Ga (average of 1.7 Ga, with most ages at 1.5–1.8 Ga) (Fig. 9).

4.1.4 North Qinling orogenic belt

The Qinling orogenic belt is located to the south of the study area and is a composite orogenic belt that was formed by the convergence of the North China and Yangtze plates. It underwent multi-stage hyperplasia and collision between different continental blocks (Dong and Santosh, 2016; Wang et al., 2015; Wang T et al., 2009; Meng and Zhang, 1999). Many Neoproterozoic granitic rocks that range in age from 979 to 815 Ma are distributed in the Northern Qinling orogenic belt (Wang et al., 2015; Zheng et al., 2013). They are related to the accumulation and breakup of the Rodinia supercontinent, which may reflect Neoproterozoic tectonomagmatic events in the ancient Qinling Block. During the Paleozoic, the Qinling Ocean experienced subduction, hyperplasia, and collision, producing a large number of tectonomagmatic thermal events that were accompanied by granite intrusions. These events can be divided into three age groups: 505–470, 455–422, and 415–400 Ma (Wang F et al., 2009; Ratschbacher et al., 2003). During the Early Mesozoic, the tectonic setting in the Mianlue Ocean changed from subduction to closure. The collision between the Yangtze Craton and the Qinling Block was accompanied by the intrusion of a large number of granites, which can be divided into two groups: 250–235 and 235–185 Ma. Granitic magmatism of the Late Mesozoic occurred at 160–130 and 120–100 Ma, and was related to the remote continental margin or the intracontinental effect due to the subduction of the paleo-Pacific Ocean (Qin et al., 2015; Wang X X et al., 2015; Wang T et al., 2009).

The $\epsilon_{\text{Hf}}(t)$ values of Early Paleozoic magmatism ranged from -13.8 to 13.3 (average of 0.3, with uniformly distributed positive and negative values), while the corresponding T_{DM2} ages were between 0.6 and 2.4 Ga (average of 1.4 Ga, with ages concentrated at 0.8–1.1 and 1.4–2.0 Ga). The $\epsilon_{\text{Hf}}(t)$ values of Meso–Neoproterozoic magmatism ranged from -16 to 13 (average of -0.6, with most values < 0), while the T_{DM2} ages were between 0.8 and 2.7 Ga (average of 1.8 Ga, with most ages at 1.6–2.0 Ga). The $\epsilon_{\text{Hf}}(t)$ values of the Early Paleoproterozoic ranged from -5.4 to 5.5 (average of -1.5, with most values < 0), and the T_{DM2} ages were between 2.7 and 3.3 Ga (average of 3.1 Ga, with most ages at 3.0–3.3 Ga) (Fig. 9).

4.2 Primary Provenance

4.2.1 Middle Jurassic Zhiluo Formation

The samples from the Zhiluo Formation had two main peak ages: Late Paleozoic and Late Paleoproterozoic, with a weak peak age during the Early Paleozoic. The zircon ages of the Late Paleozoic (250–330 Ma, 34%) matched the peak magmatic rock ages in the eastern parts of the Alxa and Yinshan blocks, which are speculated to be the main sources (Figs. 6, 8). Permian–Triassic granites and metamorphic rocks are widely distributed in the Alxa Block (Xie et al., 2020; Zhang J J et al., 2019; Gong et al., 2018; Lei et al., 2017). The Yinshan Block also contains many Permian–Triassic magmatic rocks (Feng et al., 2020; Zheng et al., 2019; Zhou Q et al., 2018; Zhang X et al., 2018; Sun D et al., 2017). The $\epsilon_{\text{Hf}}(t)$ values of the zircons from the Late Paleozoic sample were evenly positive and negative, ranging from -12.7 to 9.9, and the T_{DM2} ages varied widely (0.7–2.1 Ga). The Hf isotopes of the samples were consistent with the Hf isotopic characteristics of the Alxa and Yinshan blocks and could not be clearly distinguished (Fig. 9). In addition, Zhang et al. (2016) reported that the ages of the intrusive diabase were 277.2 ± 2.8 and 276.3 ± 7.6 Ma in the Hexi Corridor area, but the exposure was small and unlikely to provide a large number of Permian zircons.

Early Paleozoic (420–500 Ma, 15%) zircons were most likely derived from the Early Paleozoic magmatic rocks that are widely distributed in the North Qilian orogenic belt and the western part of the North Qinling orogenic belt (Zhang X Y et al., 2019; Sun X L et al., 2017; Zhang et al., 2017; Yang H et al., 2015). However, the peak age of the Early Paleozoic zircons from the Alxa Block was 375 Ma, which is inconsistent with the 450 Ma peak of the Early Paleozoic zircons from the study area. The $\epsilon_{\text{Hf}}(t)$ values of the Early Paleozoic zircons were both positive and negative, ranging from -12.4 to 11.3, and most of the T_{DM2} ages were between 1.4 and 2.2 Ga. The Hf isotopic characteristics of the samples in this study were consistent with those of the North Qilian and North Qinling orogenic belts, and could not be clearly distinguished.

Late Paleoproterozoic (1 720–2 000 Ma, 25%) and Early Paleoproterozoic (2 340–2 580 Ma, 7%) rocks are widely exposed in the surrounding tectonic units, which generally showed two peak ages at 1 800 and 2 500 Ma, both of which exhibited good comparability. Including the Kunzite belt in the Yinshan Block (Ouyang et al., 2020; Chen et al., 2017; Su et al., 2014; Bao et al., 2013; Dong et al., 2013; Ma et al., 2013a), metamorphic crystalline basement is found in the eastern part of the Alxa Block (Dan et al., 2014; Geng and Zhou, 2011, 2010; Geng et al., 2010; Li et al., 2004). The Paleoproterozoic orogenic events related to the North China Craton have regional characteristics, which provide evidence of the Proterozoic Helan Depression and the concentrated structures related to the breakup of the Columbia supercontinent in China (Gao et al., 2013; Zhai and Peng, 2007; Darby and Gehrels, 2006). In comparison, the peak age of Early Paleoproterozoic zircons in the Alashan Block is younger (2 335 Ma), while the distribution of Early Paleoproterozoic zircons in the Yinshan Block is consistent with that of the study area (Fig. 8). The Late Paleoproterozoic zircons had $\epsilon_{\text{Hf}}(t)$ values ranging from -1.4 to 10.1 (only one zircon had an $\epsilon_{\text{Hf}}(t)$ value of 20) and T_{DM2} ages at 2.6–3.2

Ga, which were inconsistent with the Hf isotopic characteristics (most $\epsilon_{\text{Hf}}(t)$ values were >0 , with T_{DM2} ages at 1.4–1.7 Ga) of the Alxa Block, but consistent with the Hf isotopic characteristics of the Yinshan Block. Therefore, the Late Paleoproterozoic zircons were likely derived from the Yinshan Block. The $\epsilon_{\text{Hf}}(t)$ values of the Early Paleoproterozoic zircons ranged from 6.0 to 9.7 (i.e., >0), while the corresponding T_{DM2} ages were between 2.5 and 2.7 Ga, which were inconsistent with the Hf isotopic characteristics of the North Qinling orogenic belt (most $\epsilon_{\text{Hf}}(t)$ values were <0 and the T_{DM2} ages were concentrated at 3.0–3.3 Ga), but consistent with the Hf isotopic characteristics of the Yinshan Block. Therefore, the Early Paleoproterozoic zircons were mainly derived from the Yinshan Block.

In addition, Late Mesoproterozoic to Early Neoproterozoic (770–1 100 Ma, 7%) zircons have been reported to be widely distributed in the western part of the North Qinling orogenic belt (Sun D et al., 2017; Shi et al., 2013; Yang et al., 2010), and are partly exposed in the eastern part of the North Qilian orogenic belt (Zhang J Y et al., 2019; Yang F et al., 2015; Xu et al., 2008), both of which contributed to the sediment provenance in the study area. Large-scale magmatism in the Qilian-Qinling junction was related to the convergence and breakup of the Rodinia supercontinent during this period (Pei et al., 2012; Xu et al., 2008). The peak zircon ages in the Northern Qilian orogenic belt are significantly younger (846 Ma), while the age distribution of zircons in the western part of the Northern Qinling orogenic belt is consistent with that of the study area. The $\epsilon_{\text{Hf}}(t)$ values of the Late Mesoproterozoic–Early Neoproterozoic zircons were relatively even positive and negative values, with T_{DM2} ages ranging from 1.5 to 2.3 Ga. These values are consistent with the Hf isotopic characteristics of the Northern Qinling orogenic belt, but inconsistent with the T_{DM2} ages concentrated at 1.5–1.8 Ga in the North Qilian orogenic belt. Therefore, the Late Mesoproterozoic–Early Neoproterozoic zircons were mainly derived from the North Qinling orogenic belt.

In summary, the zircons from the Zhiluo Formation (Late Paleozoic, Late Paleoproterozoic, and Early Paleoproterozoic) were mainly derived from the crystalline basement series (Khondalites, intermediate-acid intrusive rocks, and metamorphic rocks) of the Alashan Block to the northwest and the Yinshan Block to the north. A few zircons (Early Paleozoic and late Middle Proterozoic–Early Neoproterozoic) were derived from Caledonian magmatic rocks and Jingning Period rocks from the western part of the Northern Qilian Orogenic Belt to the west and the Northern Qinling orogenic belt to the south.

During the depositional stage of the Zhiluo Formation, the deposition range of the Ordos Basin was much larger than that of the present, and the depocenter was located in the southern part of the basin, with a high northern and low southern topography (Zhao H L et al., 2020; Zhao J F et al., 2010). The southwestern margin of the basin was restricted by paleo-topography and located in the provenance intersection region, where the sources from the southern area only affected the zircon age groups of the perimeter of the paleo-channels. The Northern Qilian orogenic belt provided the main provenance of the Zhiluo Formation in the southern part of the basin (Lei et al., 2017), while the northern Yinshan Block and Alxa Block provided the main provenance of the western margin (Yu et al.,

2020; Guo et al., 2018a; Guo et al., 2010). Where the rivers converge, the northern sources are dominant and contain some of the southern sources. This understanding is consistent with previous analyses of the Zhiluo Formation in the surrounding regions, which showed that the dominant transport directions were mainly southward and southeastward based on analyses of the paleocurrents, detrital zircons and heavy minerals (Yu et al., 2020; Zhao H L et al., 2020; Guo et al., 2018a; Lei et al., 2017; Zhao J F et al., 2010).

4.2.2 Middle Jurassic Anding Formation

The peak ages of the zircons from the Anding Formation were the same as those from the Zhiluo Formation, but the proportion of the main peak differed. The age of the main peak was of the Late Paleoproterozoic (35%), while the ages of the secondary peaks were of the Late Paleozoic (18%), Early Paleozoic (21%), and Early Paleoproterozoic (13%), with minor peaks in the Late Mesoproterozoic–Early Neoproterozoic. As mentioned above, most of the sediments of the Anding Formation (Late Paleozoic, Late Paleoproterozoic, and Early Paleoproterozoic) were derived from the Alashan Block to the northwest and the Yinshan Block to the north, while a few zircons (Early Paleozoic and Late Middle Proterozoic–Early Neoproterozoic) were derived from the western part of the Northern Qilian orogenic belt to the west and the Northern Qinling orogenic belt to the south. It is worth noting that four zircons that did not have ages in the peak age range were present in the Anding Formation, all of which were of Cryptozoic age. The overall proportion of Paleoproterozoic zircons increased significantly, and the Paleozoic zircons were relatively depleted and removed from older basement rocks. The metamorphic zircons were dated at 2 972 Ma, which likely corresponds to the age of the ancient metamorphic basement rocks in different areas of the Alxa Block, for example, zircons from gneisses in the Alxa Left Banner area (2 914±11 Ma) (Geng et al., 2007), zircons from biotite gneisses in the Helanshan area (2 839±11 Ma, based on secondary ion mass spectrometry (SIMS) analyses) (Dan et al., 2012), and zircons from mica-gneiss in the Helanshan area (2 871±23 Ma, based on sensitive high-resolution ion microprobe (SHRIMP) analysis) (Dong et al., 2007). The ages of two zircons (1 529 and 1 515 Ma) likely correspond to the basement ages of the Qinling terrane in the North Qinling orogenic belt. Previous U-Pb analyses of single zircons from the Qinling terrane yielded ages ranging from 1 400 to 1 600 Ma, which recorded major magmatism of the initial phase (Cao et al., 2017; Shi et al., 2013; Yang et al., 2010; Lu et al., 2009). A metamorphic zircon dated at 660 Ma was probably derived from the ophiolite and rift valley volcanics in the western part of North Qilian orogenic belt (Xia et al., 2016; Xu et al., 2009; Tseng et al., 2007; Shi et al., 2004; Guo et al., 2002; Mao et al., 1998).

4.2.3 Lower Cretaceous Luohe and Huanhe-Huachi formations

The distribution of detrital zircon peak ages in the Lower Cretaceous Luohe and Huanhe-Huachi formations were essentially the same, except for some differences in the peak proportions of the Paleozoic zircons; thus, the two formations are dis-

crossed together. The peak age distribution of the detrital zircons was the same as that of the Zhiluo Formation, with the following peak ages: Early Paleozoic, Late Paleozoic, Late Proterozoic, and Early Proterozoic, with very few peaks during the Late Mesoproterozoic–Early Neoproterozoic. However, Early Paleozoic zircons dominated the Luohe Formation, while Late Paleozoic zircons dominated the Huanhe-Huachi Formation. Most of the zircons were derived from the Alashan Block to the northwest and the Yinshan Block to the north, while a few were derived from the western part of the Northern Qilian orogenic belt to the west and the Northern Qinling orogenic belt to the south. Notably, zircon ages before 250 Ma first appeared in these two formations, including two from the Luohe Formation (223 and 246 Ma) and four from the Huanhe-Huachi Formation (144, 209, 238, and 243 Ma). Except for the 144 Ma zircon (i.e., Early Cretaceous), all the zircons were from the Triassic. Early Mesozoic magmatism developed widely in the Qinling orogenic belt and was dominated by continental collision. A large number of Triassic intrusive granites are distributed in the western part of the North Qinling orogenic belt and magmatism can be divided into two stages: 250–235 and 235–185 Ma (Dong and Santosh, 2016; Wang X X et al., 2015; Dong et al., 2012; Ding et al., 2011; Jiang et al., 2010; Wang et al., 2007). Therefore, we speculate that the source of these two formations was mainly the western part of the North Qinling orogenic belt. An Early Cretaceous zircon age (144 Ma) was also obtained from a magmatic zircon in the Huanhe-Huachi Formation. Late Mesozoic granitic magmatism in the North Qinling area also occurred, for which batholith zircon U-Pb ages showed peaks at 158, 145, and 124 Ma (Wang X X et al., 2015, 2011; Yang et al., 2014; Qin et al., 2012). A large number of acidic intrusive bodies with emplacement ages at 142–149 Ma have been observed in the Xiaoshan area of the North Qinling orogenic belt (Liang et al., 2020; Lu and Liang, 2018; Li et al., 2013; Zeng et al., 2013; Hu et al., 2011), thus, this Early Cretaceous zircon presumably originated from the granite rocks in this region.

4.3 Analysis of Zircon U-Pb Age Changes

When analyzing the provenance of detrital zircons, not only should the age distributions of the surrounding rock bodies be identified, but the spectral distributions of the detrital zircons in the underlying strata should also be investigated; otherwise, incorrect interpretations could occur (Pereira et al., 2016; Gehrels et al., 2011; Thomas et al., 2011; Dickinson and Gehrels, 2009; Link et al., 2005). Previous studies demonstrated that the Yan'an Formation sandstone is a recycled deposit that was laid after the stratum was uplifted and eroded prior to the Jurassic along the western margin of the Ordos Basin (Guo et al., 2018a, b). In this regard, the U-Pb ages of the Late Triassic–Middle Jurassic detrital zircons along the southwestern and western margins of the Ordos Basin are statistics (Figs. 6 and 10). Compared to the underlying Yan'an and Yanchang formations, the Zhiluo Formation had a relatively obvious Permian peak age group; however, the Proterozoic peak age group was greatly reduced, which rules out the possibility that the sandstone in the Zhiluo Formation is a recycled deposit. Therefore, the provenance of the Zhiluo Formation inferred from the detri-

tal zircon ages is correct. In addition, these areas are located in close proximity. From the Late Triassic–Middle Jurassic, the number of detrital zircons in the samples dated at ~440 Ma and ~1 000 Ma increased markedly, while the number of zircons dated at ~1 900 and ~2 500 Ma detrital zircons decreased, thus suggesting that the provenance of the Qinling orogen increased obviously. This may have been the response of the main collision between the South China Craton and North China Craton, which occurred during the Late Triassic (Wang X X et al., 2015; Bao et al., 2014; Dong et al., 2011).

The Zhiluo and Anding formations were continuously deposited in most areas of the basin, and no related tectonic events have been observed. According to the detrital zircon spectrum, there is a considerable difference between the two formations, with the Early Paleozoic and Proterozoic ages increasing significantly. This was likely affected by climate change for the following reasons: the sediments of the Anding Formation are mainly amaranth, while the underlying Zhiluo Formation is mainly gray-green (Fig. 2). A set of micritic carbonates are developed in the Anding Formation throughout the region, the overall background is a salty lacustrine environment, and the grain size of the sediments is fine, reflecting a significant decrease in the supply of terrigenous clastic materials. The climate during the deposition of the Yan'an and Zhiluo formations was generally warm and humid, while the climate during the deposition of the Anding Formation was dry and cold, indicating a change in the paleoclimatic environment (Yi et al., 2019; Guo et al., 2018b; Sun X L et al., 2017; Li et al., 2015, 2014; Liu and Yang, 2000). In recent years, climatic controls on changes in sediment provenance have been widely observed (Litty et al., 2017; Bekaddour et al., 2014; Steffen et al., 2010). A dry and cold climate led to a reduction in the amount of denudation of exposed rocks at the surface, thereby weakening (enhancing) the contribution of zircons from Paleozoic granites (Proterozoic basement rocks).

The Lower Cretaceous Luohe and Huanhe-Huachi formations and the underlying Middle Jurassic strata differed significantly because there were more zircon ages dated at <250 Ma (209–246 and 144 Ma), which were probably all derived from the North Qinling orogenic belt. According to their statistics, the upper Triassic and Middle Jurassic strata on the periphery did not contribute zircons to this group (Figs. 6, 10). Although some detrital zircons have been recorded at this age, the overall number is relatively small (Guo et al., 2017; Bao et al., 2014; Xie and Heller, 2013), indicating that the Indosinian granite in the North Qinling orogenic belt may have only been partially exposed before the Early Cretaceous; thus, it contributed little to the provenance. Among the zircon ages of the Luohe Formation, the proportion of Early Paleozoic zircons increased significantly and showed a strong main peak at ~436 Ma, while zircons of the remaining age groups decreased obviously; hence, the provenances of the North Qinling orogen or North Qilian orogenic belt clearly increased. Most of the zircons were angular with a low roundness, indicating that they were not transported for a long distance by recycled deposits. This indicates a very low possibility for a recycled deposit. In the core, conglomerate beds of the Middle Jurassic Fenfanghe Formation (no samples) were observed along with several sets

of huge gravel conglomerate beds in the Luohe Formation, suggesting an intense tectonic movement at the margin of the basin during the Late Jurassic–Early Cretaceous. From the Late Jurassic to Early Cretaceous, the Qinling–Qilian orogenic belt underwent a strong multi-cycle intracontinental orogeny. Yanshanian granites are widely distributed in the North Qinling orogenic belt, and a set of alluvial conglomerates of the Yijun Formation were deposited along the southern margin of the basin, which was derived mainly from the North Qinling region. This suggests that the tectonic activity was relatively strong in the North Qinling area (Qi et al., 2017; Wang X X et al., 2015; Wang J Q, 2010; Liu et al., 2006), which may have caused the Indosinian granites to become more widely exposed and undergo weathering denudation, thus increasing the amount of source material from the Indo-Chinese granites contributing to the strata in the study area.

4.4 Uranium Source and Metallogensis

For sandstone-type uranium deposits, a source area sufficiently rich in uranium is required for the development of uranium ore deposits, and intermediate-acid magmatic rocks are

the best uranium-containing sources. Previous studies have shown that Paleozoic–Mesozoic magmatic rocks with high uranium contents around the Ordos Basin are the main source of uranium to the sandstone-type uranium deposits in the basin (Akhtar et al., 2017; Wang et al., 2011; Li et al., 2010). The analysis of the provenance in this study shows that the main source areas for the southwest margin of the basin are the Alxa and Yinshan blocks, with contributions from the North Qilian–North Qinling orogenic belts. The Alxa Block has undergone two crustal accretion events and multiple phases of magmatism, and Late Paleozoic granites are the most widely distributed granites (Dan et al., 2016; Luo, 2015; Windley et al., 2007; Zhou and Yu, 1989). The rock types exposed at the surface are mainly alkaline granites, granodiorites, migmatite granites, and granitic gneisses, and the uranium content of the rocks in the source area is generally high. In addition, in the Yinshan orogenic belt to the north of the Ordos Basin, the gneiss group of the Archean Eonothem Wulashan terrane also has a high uranium content and experienced acidic magmatic intrusion that led to uranium enrichment during the Indosinian and Yanshanian. The average uranium content of Paleozoic granite bodies can

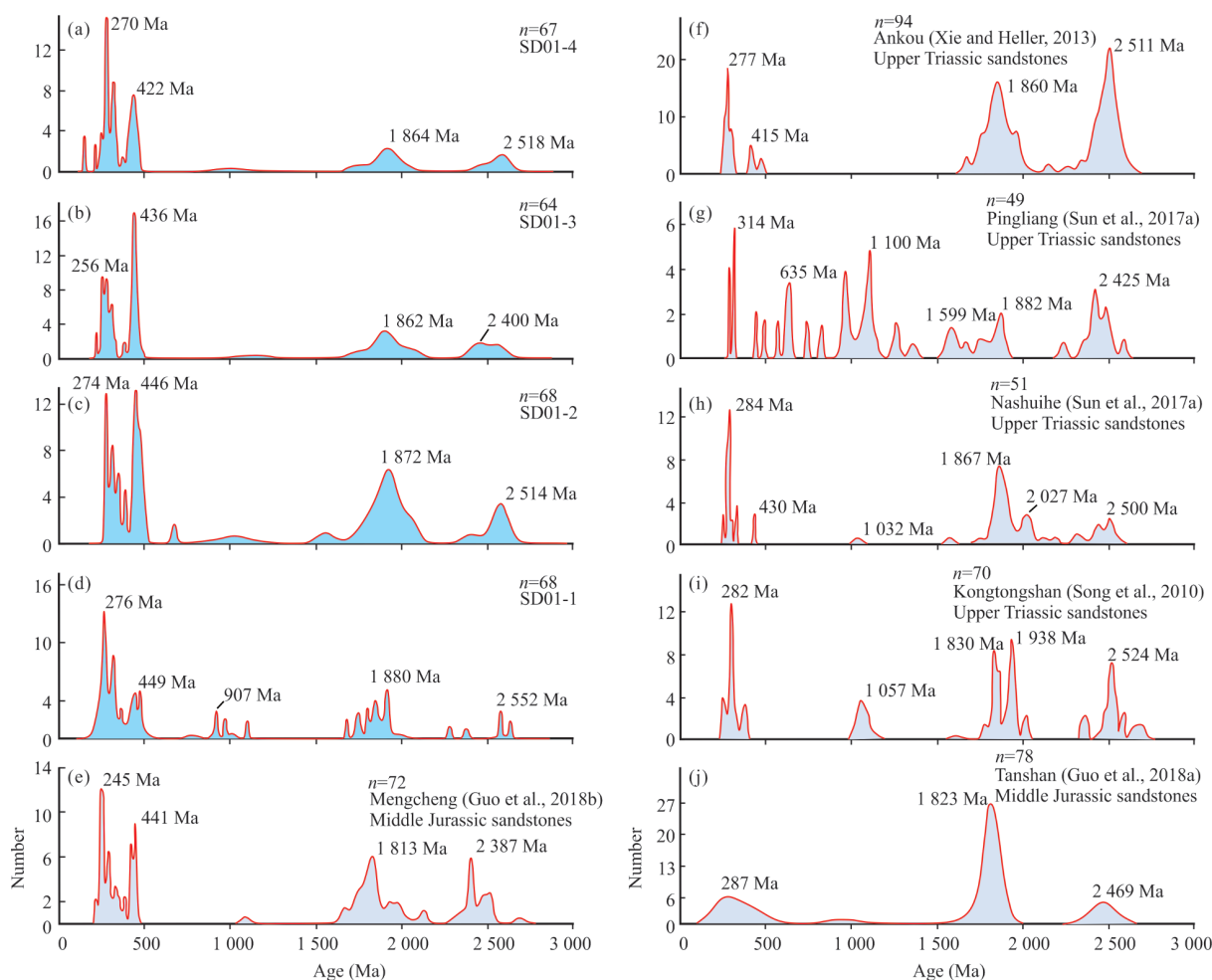


Figure 10. Relative age probability diagram comparing ages of zircon grains. U-Pb age histograms of the detrital zircons from the Paleozoic sandstones in the southwest Ordos Basin. (a)–(d) is the test sample, and (e)–(j) are collected from the west and southwest of Ordos Basin (sample locations are plotted on the Fig. 1); (e) the Yanan Formation of Middle Jurassic in Mengcheng area (Guo et al., 2018b); (j) the Yan'an Formation of Middle Jurassic in Tanshan area (Guo et al., 2018a); (f) Yanchang Formation of Upper Triassic in Ankou area (Xie and Heller, 2013); (g)–(h) Upper Triassic Yanchang Formation in Pingliang and Nashuihe area (Sun D et al., 2017); (i) Upper Triassic Yanchang Formation in Kongtongshan area (Song et al., 2010).

reach 9.92×10^{-6} (Jiao et al., 2015; Wang L et al., 2015; Liu et al., 2012; Li et al., 2008). The uranium-bearing phosphorite of the Lower Cambrian Xinji Formation in the Longxian-Qishan area, and the Proterozoic–Paleozoic acidic magmatic rocks and mixed rocks in the North Qinling orogenic belt are also rich in uranium, with a uranium content of $\sim 2.2 \times 10^{-6}$ – 8.6×10^{-6} (Zhang et al., 2018). Therefore, a large number of uranium-rich rocks in the source area provide a good uranium source for the formation of sandstone-type uranium deposits. In addition, during the Mesozoic–Cenozoic, the western Ordos Basin underwent multiple periods of tectonic compression, which facilitated the uplift and exposure of uranium-rich rocks at the bottom of the basin. During the sedimentation period, or the infiltration and transformation periods of the target layer, the coupled effects of these two factors provided sufficient internal and external uranium sources to the basin when the orogenic conditions were favorable (Akhtar et al., 2017; Liu et al., 2013; Guo et al., 2010; Liu et al., 2006).

5 CONCLUSIONS

(1) The U–Pb ages of Middle Jurassic–Lower Cretaceous detrital zircons from the Zhenyuan area along the southwestern margin of the Ordos Basin showed four peak ages at 250–330, 420–500, 1 720–2 000, and 2 340–2 580 Ma, with a small number of zircons dated at 770–1 100 Ma. The overall distribution of the ages was relatively consistent, but the main peaks in each stratum differed. Most zircons were of the Paleozoic and Late Paleoproterozoic, while only a few were of the Early Paleoproterozoic and Late Mesoproterozoic–Early Neoproterozoic.

(2) Comparing the isotopic chronologies of the study area with those of the periphery revealed that the main source of the Late Mesozoic strata (Late Paleozoic, Late Paleoproterozoic, and Early Paleoproterozoic zircons) was the crystalline basement series (Khondalites, intermediate-acid intrusive rocks, and metamorphic rocks) of the Alashan Block to the northwest and the Yinshan Block to the north, with smaller contributions (Early Paleozoic and Late Mesoproterozoic–Early Neoproterozoic zircons) from Caledonian magmatic rocks and Jingning Period rocks from the western part of the Northern Qilian orogenic belt to the west and the northern Qinling orogenic belt to the south.

(3) The age composition changes in the Anding Formation were likely affected by climatic changes during the Middle–Late Jurassic. In addition, Triassic age zircons (<250 Ma) were first observed in Early Cretaceous strata, suggesting that the North Qinling region was tectonically active during the Late Jurassic, which exposed the Indosinian granites more extensively at the surface and provided a source of basin sediments.

(4) The provenance of the Luohe Formation, which contains the ore-bearing horizon, was mainly from the intermediate-acid intrusive rocks and metamorphic rocks of the Alxa Block to the northwest; gneisses, granulites, and Khondalites from the Yinshan area to the north; a large number of Hercynian igneous rocks; and partly from the intermediate-acid intrusive rocks, basic intrusive rocks, and metamorphic rocks of the North Qilian–North Qinling orogenic belts. It may not be sufficient to identify provenance based on detrital zircons alone, and other provenance analysis methods should be integrated in

future studies to determine the source of basin sediments more accurately.

ACKNOWLEDGMENTS

We are grateful to Dr. Zijian Wang for helping on the LA-ICP-MS U–Pb dating and data process. We thank teacher Fang Xiang for her constructive comments. This study is supported by the National Key Research and Development Program of China (No. 2018YFC604201) and the International Geoscience Programme (No. IGCP675). The final publication is available at Springer via <https://doi.org/10.1007/s12583-021-1450-y>.

Electronic Supplementary Materials: Supplementary materials (Tables S1, S2) are available in the online version of this article at <https://doi.org/10.1007/s12583-021-1450-y>.

REFERENCES CITED

- Akhtar, S., Yang, X. Y., Pirajno, F., 2017. Sandstone Type Uranium Deposits in the Ordos Basin, Northwest China: A Case Study and an Overview. *Journal of Asian Earth Sciences*, 146: 367–382. <https://doi.org/10.1016/j.jseas.2017.05.028>
- Amelin, Y., Lee, D. C., Halliday, A. N., et al., 1999. Nature of the Earth's Earliest Crust from Hafnium Isotopes in Single Detrital Zircons. *Nature*, 399(6733): 252–255. <https://doi.org/10.1038/20426>
- Andersen, T., 2002. Correction of Common Lead in U–Pb Analyses that do not Report ^{204}Pb . *Chemical Geology*, 192(1/2): 59–79. [https://doi.org/10.1016/s0009-2541\(02\)00195-x](https://doi.org/10.1016/s0009-2541(02)00195-x)
- Bao, C., Chen, Y. L., Li, D. P., 2013. LA-MC-ICP-MS Zircons U–Pb Dating and Hf Isotopic Compositions of the Paleoproterozoic Amphibolite in Bayan Ul Area, Inner Mongolia. *Geological Bulletin of China*, 32(10): 1513–1524 (in Chinese with English Abstract)
- Bao, C., Chen, Y. L., Li, D. P., et al., 2014. Provenances of the Mesozoic Sediments in the Ordos Basin and Implications for Collision between the North China Craton (NCC) and the South China Craton (SCC). *Journal of Asian Earth Sciences*, 96: 296–307. <https://doi.org/10.1016/j.jseas.2014.09.006>
- Bekaddour, T., Schlunegger, F., Vogel, H., et al., 2014. Paleo Erosion Rates and Climate Shifts Recorded by Quaternary Cut-and-Fill Sequences in the Pisco Valley, Central Peru. *Earth and Planetary Science Letters*, 390: 103–115. <https://doi.org/10.1016/j.epsl.2013.12.048>
- Blichert-Toft, J., Albarède, F., 1997. The Lu–Hf Isotope Geochemistry of Chondrites and the Evolution of the Mantle–Crust System. *Earth and Planetary Science Letters*, 148(1/2): 243–258. [https://doi.org/10.1016/S0012-821x\(97\)00040-x](https://doi.org/10.1016/S0012-821x(97)00040-x)
- Bonnetti, C., Cuney, M., Michels, R., et al., 2015. The Multiple Roles of Sulfate-Reducing Bacteria and Fe–Ti Oxides in the Genesis of the Bayinwula Roll Front-Type Uranium Deposit, Erlian Basin, NE China. *Economic Geology*, 110(4): 1059–1081. <https://doi.org/10.2113/econgeo.110.4.1059>
- Cao, H. H., Li, S. Z., Zhao, S. J., et al., 2017. Precambrian Tectonic Affinity of the North Qinling Microcontinent: Constraints from the Discovery of Mesoproterozoic Magmatic Zircons in the Qinling Group. *Geological Journal*, 52: 142–154. <https://doi.org/10.1002/gj.2997>
- Chen, A. Q., Zhang, X. X., Mi, W. T., et al., 2019. Favorable Sandstone Reservoir Characteristics and Hydrocarbon Accumulation Models of Middle Jurassic Zhiluo Formation in the Southwestern Ordos Basin, China. *Journal of Earth Sciences and Environment*, 41(5): 517–528 (in Chinese with English Abstract)

- Chen, N. H. C., Zhao, G. C., Jahn, B. M., et al., 2017. U-Pb Zircon Ages and Hf Isotopes of ~2.5 Ga Granitoids from the Yinshan Block, North China Craton: Implications for Crustal Growth. *Precambrian Research*, 303: 171–182. <https://doi.org/10.1016/j.precamres.2017.03.016>
- Chen, Y. X., Song, S. G., Niu, Y. L., et al., 2014. Melting of Continental Crust during Subduction Initiation: A Case Study from the Chaidanuo Peraluminous Granite in the North Qilian Suture Zone. *Geochimica et Cosmochimica Acta*, 132: 311 – 336. <https://doi.org/10.1016/j.gca.2014.02.011>
- Cherniak, D. J., Watson, E. B., 2001. Pb Diffusion in Zircon. *Chemical Geology*, 172(1/2): 5 – 24. [https://doi.org/10.1016/s0009-2541\(00\)00233-3](https://doi.org/10.1016/s0009-2541(00)00233-3)
- Dan, W., Li, X. H., Guo, J. H., et al., 2012. Integrated *in situ* Zircon U-Pb Age and Hf-O Isotopes for the Helanshan Khondalites in North China Craton: Juvenile Crustal Materials Deposited in Active or Passive Continental Margin? *Precambrian Research*, 222/223: 143–158. <https://doi.org/10.1016/j.precamres.2011.07.016>
- Dan, W., Li, X. H., Wang, Q., et al., 2014. An Early Permian (ca. 280 Ma) Silicic Igneous Province in the Alxa Block, NW China: A Magmatic Flare-Up Triggered by a Mantle-Plume? *Lithos*, 204: 144–158. <https://doi.org/10.1016/j.lithos.2014.01.018>
- Dan, W., Li, X. H., Wang, Q., et al., 2016. Phanerozoic Amalgamation of the Alxa Block and North China Craton: Evidence from Paleozoic Granitoids, U-Pb Geochronology and Sr-Nd-Pb-Hf-O Isotope Geochemistry. *Gondwana Research*, 32: 105 – 121. <https://doi.org/10.1016/j.gr.2015.02.011>
- Darby, B. J., Gehrels, G., 2006. Detrital Zircon Reference for the North China Block. *Journal of Asian Earth Sciences*, 26(6): 637–648. <https://doi.org/10.1016/j.jseas.2004.12.005>
- Davis, G. A., Wang, C., Zheng, Y. D., et al., 1998. The Enigmatic Yinshan Fold-and-Thrust Belt of Northern China: New Views on Its Intraplate Contractional Styles. *Geology*, 26(1): 43. [https://doi.org/10.1130/0091-7613\(1998\)0260043:teyfat>2.3.co;2](https://doi.org/10.1130/0091-7613(1998)0260043:teyfat>2.3.co;2)
- Dickinson, W. R., Gehrels, G. E., 2008. Sediment Delivery to the Cordilleran Foreland Basin: Insights from U-Pb Ages of Detrital Zircons in Upper Jurassic and Cretaceous Strata of the Colorado Plateau. *American Journal of Science*, 308(10): 1041–1082. <https://doi.org/10.2475/01.2008.01>
- Ding, L. X., Ma, C. Q., Li, J. W., et al., 2011. Timing and Genesis of the Adakitic and Shoshonitic Intrusions in the Laoniushan Complex, Southern Margin of the North China Craton: Implications for Post-Collisional Magmatism Associated with the Qinling Orogen. *Lithos*, 126(3/4): 212–232. <https://doi.org/10.1016/j.lithos.2011.07.008>
- Dong, C. Y., Liu, D. Y., Li, J. J., et al., 2007. Paleoproterozoic Khondalite Belt in the Western North China Craton: New Evidence from SHRIMP Dating and Hf Isotope Composition of Zircons from Metamorphic Rocks in the Bayan Ul-Helanshan Area. *Chinese Science Bulletin*, 52 (21): 2984–2993 (in Chinese with English Abstract)
- Dong, C. Y., Wan, Y. S., Xu, Z. Y., et al., 2013. SHRIMP Zircon U-Pb Dating of Late Paleoproterozoic Kandalites in the Daqing Mountains Area on the North China Craton. *Science China Earth Sciences*, 56(1): 115–125. <https://doi.org/10.1007/s11430-012-4459-3>
- Dong, Y. P., Liu, X. M., Zhang, G. W., et al., 2012. Triassic Diorites and Granitoids in the Foping Area: Constraints on the Conversion from Subduction to Collision in the Qinling Orogen, China. *Journal of Asian Earth Sciences*, 47: 123–142. <https://doi.org/10.1016/j.jseas.2011.06.005>
- Dong, Y. P., Santosh, M., 2016. Tectonic Architecture and Multiple Orogeny of the Qinling Orogenic Belt, Central China. *Gondwana Research*, 29(1): 1–40. <https://doi.org/10.1016/j.gr.2015.06.009>
- Feng, F., Xu, Z. Y., Dong, X. J., et al., 2020. LA-ICP-MS Zircon U-Pb Dating, Hf Isotopic Compositions of Granite Porphyry in Wenduermiao-Jining Area, Inner Mongolia and Its Geological Significance. *Earth Science*, <http://kns.cnki.net/kcms/detail/42.1874.P20200116.1456.002.html> (in Chinese with English Abstract)
- Fu, Y., Wei, S. C., Jin, R. S., et al., 2016. Current Status and Existing Problems of China's Sandstone-Type Uranium Deposits. *Acta Geologica Sinica*, 90(12): 3519–3544 (in Chinese with English Abstract)
- Gao, S. L., Lin, J. Y., Lu, Y. J., 2013. Formation Epoch and Its Geological Implication of Paleoproterozoic A-Type Granite in Shizuizi of Jingyuan County, Ningxia Provenance. *Acta Petrologica Sinica*, 29(8): 2676–2684 (in Chinese with English Abstract)
- Gehrels, G. E., Blakey, R., Karlstrom, K. E., et al., 2011. Detrital Zircon U-Pb Geochronology of Paleozoic Strata in the Grand Canyon, Arizona. *Lithosphere*, 3(3): 183–200. <https://doi.org/10.1130/1121.1>
- Geng, Y. Y., Liu, Z. Y., He, Z. B., et al., 2020. Provenance and Ore-Forming Tectonic Setting of Sandstone-Type Uranium Deposits in the Southern Margin of Junggar Basin—Insights from U-Pb Ages and Hf Isotopes of Detrital Zircons. *Geological Review*, 66(2): 393–408 (in Chinese with English Abstract)
- Geng, Y. S., Zhou, X. W., 2011. Characteristics of Geochemistry and Zircon Hf Isotope of the Early Neoproterozoic Granite in Alax Area, Inner Mongolia. *Acta Petrologica Sinica*, 27(4): 897–908 (in Chinese with English Abstract)
- Geng, Y. S., Zhou, X. W., 2012. Early Permian Magmatic Events in the Alxa Metamorphic Basement: Evidence from Geochronology. *Acta Petrologica Sinica*, 28(9): 2667 – 2685 (in Chinese with English Abstract)
- Geng, Y. S., Wang, X. S., Shen, Q. H., et al., 2007. Chronology of the Precambrian Metamorphic Series in the Alxa Area, Inner Mongolia. *Geology in China*, 34(2): 251–261 (in Chinese with English Abstract)
- Geng, Y. S., Wang, X. S., Wu, C. M., et al., 2010. Late-Paleoproterozoic Tectonothermal Events of the Metamorphic Basement in Alxa Area: Evidence from Geochronology. *Acta Petrologica Sinica*, 26(4): 1159–1170 (in Chinese with English Abstract)
- Geng, Y. S., Zhou, X. W., 2010. Early Neoproterozoic Granite Events in Alax Area of Inner Mongolia and Their Geological Significance: Evidence from Geochronology. *Acta Petrologica et Mineralogica*, 29 (6): 779–795 (in Chinese with English Abstract)
- Gong, J. H., Zhang, J. X., Wang, Z. Q., et al., 2018. Zircon U-Pb Dating, Hf Isotopic and Geochemical Characteristics of Two Suites of Gabbros in the Beidashan Region, Western Alxa Block: Its Implications for Evolution of the Central Asian Orogenic Belt. *Acta Geologica Sinica*, 92(7): 1369–1388 (in Chinese with English Abstract)
- Griffin, W. L., Pearson, N. J., Belousova, E., et al., 2000. The Hf Isotope Composition of Cratonic Mantle: LAM-MC-ICPMS Analysis of Zircon Megacrysts in Kimberlites. *Geochimica et Cosmochimica Acta*, 64(1): 133–147. [https://doi.org/10.1016/S0016-7037\(99\)00343-9](https://doi.org/10.1016/S0016-7037(99)00343-9)
- Guan, H., Sun, M., Wilde, S. A., et al., 2002. SHRIMP U-Pb Zircon Geochronology of the Fuping Complex: Implications for Formation and Assembly of the North China Craton. *Precambrian Research*, 113 (1/2): 1–18. [https://doi.org/10.1016/S0301-9268\(01\)00197-8](https://doi.org/10.1016/S0301-9268(01)00197-8)
- Guo, L. Y., Gan, Z. M., Li, H. M., 2002. Single-Zircon U-Pb Dating of the Liugouxia Granitic Gneiss in the Western Segment of the North Qilian Mountains. *Chinese Geology*, 29(2): 126–128 (in Chinese with English Abstract)
- Guo, P., Liu, C. Y., Wang, J. Q., et al., 2018a. Detrital-Zircon

- Geochronology of the Jurassic Coal-Bearing Strata in the Western Ordos Basin, North China: Evidences for Multi-Cycle Sedimentation. *Geoscience Frontiers*, 9(6): 1725–1743. <https://doi.org/10.1016/j.gsf.2017.11.003>
- Guo, P., Liu, C. Y., Wang, J. Q., et al., 2018b. Detrital Zircon Geochronology of the Jurassic Strata in the Western Ordos Basin, North China: Constraints on the Provenance and Its Tectonic Implication. *Geological Journal*, 53(4): 1482–1499. <https://doi.org/10.1002/gj.2968>
- Guo, Q. Y., Li, Z. Y., Yu, J. S., et al., 2010. Meso-Neozoic Structural Evolution in the Western Margin of Ordos Basin with Respect to Uranium Ore Formation. *Uranium Geology*, 26(3): 137–144 (in Chinese with English Abstract)
- Hall, S. M., Mihalasky, M. J., Tureck, K. R., et al., 2017. Corrigendum to “Genetic and Grade and Tonnage Models for Sandstone-Hosted Roll-Type Uranium Deposits, Texas Coastal Plain, USA” [Ore Geol. Rev. 80 (2017) 716–753. *Ore Geology Reviews*, 95: 1197. <https://doi.org/10.1016/j.oregeorev.2017.07.022>]
- He, W. J., 2007. Research on the Sedimentary System of Zhiluo-Anding Formation in the Southern of the Ordos Basin: [Dissertation]. Northwest University, Xi'an (in Chinese with English Abstract)
- Hoskin, P. W. O., 2003. The Composition of Zircon and Igneous and Metamorphic Petrogenesis. *Reviews in Mineralogy and Geochemistry*, 53(1): 27–62. <https://doi.org/10.2113/0530027>
- Hu, H., Li, J. W., Deng, X. D., 2011. LA-ICP-MS Zircon U-Pb Dating of Granitoid Intrusions Related to Iron-Copper Polymetallic Deposits in Luonan-Lushi Area of Southern North China Craton and Its Geological Implications. *Mineral Deposits*, 30(6): 979–1001 (in Chinese with English Abstract)
- Isachsen, Y. W., Mitcham, T. W., Wood, H. B., 1955. Age and Sedimentary Environments of Uranium Host Rocks, Colorado Plateau. *Economic Geology*, 50(2): 127–134. <https://doi.org/10.2113/gsecongeo.50.2.127>
- Jiang, Y. H., Jin, G. D., Liao, S. Y., et al., 2010. Geochemical and Sr-Nd-Hf Isotopic Constraints on the Origin of Late Triassic Granitoids from the Qinling Orogen, Central China: Implications for a Continental Arc to Continent-Continent Collision. *Lithos*, 117(1/2/3/4): 183–197. <https://doi.org/10.1016/j.lithos.2010.02.014>
- Jiao, Y. Q., Wu, L. Q., Peng, Y. B., et al., 2015. Sedimentary-Tectonic Setting of the Deposition-Type Uranium Deposits Forming in the Paleo-Asian Tectonic Domain, North China. *Earth Science Frontiers*, 22(1): 189–205 (in Chinese with English Abstract)
- Jin, R. S., Miao, P. S., Sima, X. Z., et al., 2018. New Prospecting Progress Using Information and Big Data of Coal and Oil Exploration Holes on Sandstone-Type Uranium Deposit in North China. *China Geology*, 1(1): 167–168. <https://doi.org/10.31035/cg2018017>
- Kinny, P. D., Mass, R., 2003. Lu-Hf and Sm-Nd Isotope Systems in Zircon. *Reviews in Mineralogy and Geochemistry*, 53(1): 327–341. <https://doi.org/10.2113/0530327>
- Lee, J. K. W., Williams, I. S., Ellis, D. J., 1997. Pb, U and Th Diffusion in Natural Zircon. *Nature*, 390(6656): 159–162. <https://doi.org/10.1038/36554>
- Lei, K. Y., Liu, C. Y., Zhang, L., et al., 2017. Sedimentary Provenance of Zhiluo Formation of the Middle Jurassic in the Southern Ordos Basin: Evidence from Palaeocurrent Direction and U-Pb Geochronology of Detrital Zircons. *Earth Science Frontiers*, 24(6): 254–276 (in Chinese with English Abstract)
- Li, J. J., Shen, B. F., Li, H. M., et al., 2004. Single-Zircon U-Pb Age of Granodioritic Gneiss in the Bayan Ul Area, Western Inner Mongolia. *Regional Geology of China*, 23(12): 1243–1245 (in Chinese with English Abstract)
- Li, R. X., Li, Y. Z., 2011. The Geologic Features of Mineralization at the Dongsheng Uranium Deposit in the Northern Ordos Basin (Central China). *Russian Geology and Geophysics*, 52(6): 593–602. <https://doi.org/10.1016/j.rgg.2011.05.003>
- Li, R. X., Wang, X. L., 2007. Isotope Geochemistry of Ore Fluids for the Dongsheng Sandstone-Type Uranium Deposit, China. *Chinese Journal of Geochemistry*, 26(2): 114–122. <https://doi.org/10.1007/s11631-007-0114-7>
- Li, T. G., Wu, G., Chen, Y. C., et al., 2013. Geochronology, Geochemistry and Petrogenesis of the Yinjiagou Complex in Western Henan Province, China. *Acta Geologica Sinica*, 29(1): 46–66 (in Chinese with English Abstract)
- Li, Z. H., Dong, S. W., Feng, S. B., et al., 2015. Sedimentary Response to Middle–Late Jurassic Tectonic Events in the Ordos Basin. *Acta Geoscientica Sinica*, 36(1): 22–30 (in Chinese with English Abstract)
- Li, Z. H., Dong, S. W., Qu, H. J., 2014. Timing of the Initiation of the Jurassic Yanshan Movement on the North China Craton: Evidence from Sedimentary Cycles, Heavy Minerals, Geochemistry, and Zircon U-Pb Geochronology. *International Geology Review*, 56(3): 288–312. <https://doi.org/10.1080/00206814.2013.855013>
- Li, Z. Y., Chen, A. P., Fang, X. H., et al., 2010. Origin and Superposition Metallogenic Model of the Sandstone-Type Uranium Deposit in the Northeastern Ordos Basin, China. *Acta Geologica Sinica—English Edition*, 82(4): 745–749. <https://doi.org/10.1111/j.1755-6724.2008.tb00627.x>
- Liang, T., Li, L. M., Lu, R., et al., 2020. Early Cretaceous Mafic Dikes in the Northern Qinling Orogenic Belt, Central China: Implications for Lithosphere Delamination. *Journal of Asian Earth Sciences*, 194: 104142. <https://doi.org/10.1016/j.jseas.2019.104142>
- Link, P. K., Fanning, C. M., Beranek, L. P., 2005. Reliability and Longitudinal Change of Detrital-Zircon Age Spectra in the Snake River System, Idaho and Wyoming: An Example of Reproducing the Bumpy Barcode. *Sedimentary Geology*, 182(1/2/3/4): 101–142. <https://doi.org/10.1016/j.sedgeo.2005.07.012>
- Litty, C., Lanari, P., Burn, M., et al., 2017. Climate-Controlled Shifts in Sediment Provenance Inferred from Detrital Zircon Ages, Western Peruvian Andes. *Geology*, 45(1): 59–62. <https://doi.org/10.1130/g38371.1>
- Liu, C. Y., Zhao, H. G., Gui, X. J., et al., 2006. Space-Time Coordinate of the Evolution and Reformation and Mineralization Response in Ordos Basin. *Acta Geologica Sinica*, 80(5): 617–638 (in Chinese with English Abstract)
- Liu, H. B., Xia, Y. L., Tian, S. F., 2007. Geochronological and Source Studies of Uranium Mineralization in Dongsheng. *Uranium Geology*, 23(1): 23–29 (in Chinese with English Abstract)
- Liu, K., Wang, R., Shi, W. Z., et al., 2021. Multiple Provenance System of Lower Shihezi Formation in Hangjinqi Area, Northern Ordos Basin: Evidence from Mineralogy and Detrital Zircon U-Pb Chronology. *Earth Science*, 46(2): 540–554 (in Chinese with English Abstract)
- Liu, M., Zhang, D., Xiong, G. Q., et al., 2016. Zircon U-Pb Age, Hf Isotope and Geochemistry of Carboniferous Intrusions from the Langshan Area, Inner Mongolia: Petrogenesis and Tectonic Implications. *Journal of Asian Earth Sciences*, 120: 139–158. <https://doi.org/10.1016/j.jseas.2016.01.005>
- Liu, Q., Wu, Y. B., Wang, H., et al., 2014. Zircon U-Pb Ages and Hf Isotope Compositions of Migmatites from the North Qinling Terrane and Their

- Geological Implications. *Journal of Metamorphic Geology*, 32(2): 177–193. <https://doi.org/10.1111/jmg.12065>
- Liu, S. F., Su, S., Zhang, G. W., 2013. Early Mesozoic Basin Development in North China: Indications of Cratonic Deformation. *Journal of Asian Earth Sciences*, 62: 221 – 236. <https://doi.org/10.1016/j.jseaes.2012.09.011>
- Liu, S., Yang, S., 2000. Upper Triassic–Jurassic Sequence Stratigraphy and Its Structural Controls in the Western Ordos Basin, China. *Basin Research*, 12(1): 1–18. <https://doi.org/10.1046/j.1365-2117.2000.00107.x>
- Liu, Y. F., Nie, F. J., Jiang, S. H., et al., 2012. Ore-Forming Granites from Chaganhua Molybdenum Deposit, Central Inner Mongolia, China: Geochemistry, Geochronology and Petrogenesis. *Acta Petrologica Sinica*, 28(2): 409–420 (in Chinese with English Abstract)
- Long, X. P., Yuan, C., Sun, M., et al., 2010. Detrital Zircon Ages and Hf Isotopes of the Early Paleozoic Flysch Sequence in the Chinese Altai, NW China: New Constrains on Depositional Age, Provenance and Tectonic Evolution. *Tectonophysics*, 480(1/2/3/4): 213–231. <https://doi.org/10.1016/j.tecto.2009.10.013>
- Lu, R., Liang, T., 2018. Zircon U-Pb Dating and Geochemical Features of Hangou Granitic Body in Xiaoshan Mountain, Western Henan Province, and Its Geologic Implications. *Geology in China*, 45(1): 95–109 (in Chinese with English Abstract)
- Lu, S. N., Li, H. K., Wang, H. C., et al., 2009. Detrital Zircon Population of Proterozoic Metasedimentary Strata in the Qinling-Qilian-Kunlun Orogen. *Acta Geologica Sinica*, 25(9): 303 – 310 (in Chinese with English Abstract)
- Lu, S. N., Chen, Z. H., Li, H. K., et al., 2004. Late Mesoproterozoic–Early Neoproterozoic Evolution of the Qinling Orogen. *Regional Geology of China*, 23(2): 107–112 (in Chinese with English Abstract)
- Ludwig, K. R., 2012. User's Manual for Isoplot 3.6: A Geochronological Toolkit for Microsoft Excel. Berkeley Geochronology Center, Berkeley. 1–75
- Luo, H. L., Wu, T. R., Li, Y., 2007. Geochemistry and SHRIMP Dating of the Kebu Massif from Wulatezhongqi, Inner Mongolia: Evidence for the Early Permian Underplating beneath the North China Craton. *Acta Petrologica Sinica*, 23(4): 755–766 (in Chinese with English Abstract)
- Luo, H. L., Wu, T. R., Zhao, L., 2010. Geochemistry and Tectonic Implications of the Permian I-Type Granitoids from Urad Zhongqi, Inner Mongolia. *Acta Scientiarum Naturalium Universitatis Pekinensis*, 46(5): 805–820 (in Chinese with English Abstract)
- Luo, W., 2017. Sedimentary Evolution and Provenance Analysis of the Middle Jurassic Zhiluo Formation in Majiatan-Huianbao Area, Western Ordos Basin: [Dissertation]. Northwest University, Xi'an (in Chinese with English Abstract)
- Luo, Z. B., 2015. Formation and Evolution of Early Precambrian Continental Crust in Alxa Block. *Advances in Earth Science*, 30(8): 878–890 (in Chinese with English Abstract)
- Ma, X. D., Fan, H. R., Santosh, M., et al., 2013. Geochemistry and Zircon U-Pb Chronology of Charnockites in the Yinshan Block, North China Craton: Tectonic Evolution Involving Neoproterozoic Ridge Subduction. *International Geology Review*, 55(13): 1688 – 1704. <https://doi.org/10.1080/00206814.2013.796076>
- Ma, X. D., Guo, J. H., Liu, F., et al., 2013. Zircon U-Pb Ages, Trace Elements and Nd-Hf Isotopic Geochemistry of Guyang Sanukitoids and Related Rocks: Implications for the Archean Crustal Evolution of the Yinshan Block, North China Craton. *Precambrian Research*, 230: 61–78. <https://doi.org/10.1016/j.precamres.2013.02.001>
- Mao, J. W., Zhang, Z. C., Yang, J. M., et al., 1998. Dating of Single-Grain Zircon for Precambrian Strata in Western Part of North Qilian Mountains. *Chinese Science Bulletin*, 43(15): 1289–1294. <https://doi.org/10.1007/BF02884144>
- Meng, Q. R., Zhang, G. W., 1999. Timing of Collision of the North and South China Blocks: Controversy and Reconciliation. *Geology*, 27(2): 123 – 126. [https://doi.org/10.1130/0091-7613\(1999\)0270123:tocotn>2.3.co;2](https://doi.org/10.1130/0091-7613(1999)0270123:tocotn>2.3.co;2)
- Meng, X. H., Zhang, Y., Wang, D. Y., et al., 2018. Provenance Analysis of the Late Triassic Yichuan Basin: Constraints from Zircon U-Pb Geochronology. *Open Geosciences*, 10(1): 34 – 44. <https://doi.org/10.1515/geo-2018-0003>
- Miao, P. S., Jin, R. S., Li, J. G., et al., 2020a. The First Discovery of a Large Sandstone-Type Uranium Deposit in Aeolian Depositional Environment. *Acta Geologica Sinica—English Edition*, 94(2): 583 – 584. <https://doi.org/10.1111/1755-6724.14518>
- Miao, P. S., Chen, Y., Cheng, Y. H., et al., 2020b. New Deep Exploration Discoveries of Sandstone-Type Uranium Deposits in North China. *Geotectonica et Metallogenia*, 44(4): 561 – 575 (in Chinese with English Abstract)
- Ouyang, D. J., Guo, J. H., Peng, L. O., et al., 2020. Petrogenesis and Tectonic Implications of 2.45 Ga Potassic A-Type Granite in the Daqingshan Area, Yinshan Block, North China Craton. *Precambrian Research*, 336: 105435. <https://doi.org/10.1016/j.precamres.2019.105435>
- Pei, X. Z., Ding, S. P., Li, Z. C., et al., 2007a. LA-ICP-MS Zircon U-Pb Dating of the Gabbro from the Guanzizhen Ophiolite in the Northern Margin of the Western Qinling and Its Geological Significance. *Acta Geologica Sinica*, 81(11): 1550 – 1561 (in Chinese with English Abstract)
- Pei, X. Z., Ding, S. P., Zhang, G. W., et al., 2007b. Zircons LA-ICP-MS U-Pb Dating of Neoproterozoic Granitoid Gneisses in the North Margin of West Qinling and Geological Implication. *Acta Geologica Sinica*, 81(6): 772–786 (in Chinese with English Abstract)
- Pei, X. Z., Li, Z. C., Li, R. B., et al., 2012. LA-ICP-MS U-Pb Ages of Detrital Zircons from the Meta-Detrital Rocks of the Early Palaeozoic Huluhe Group in Eastern Part of Qilian Orogenic Belt: Constraints of Material Source and Sedimentary Age. *Earth Science Frontiers*, 19(5): 205–224 (in Chinese with English Abstract)
- Pereira, M. F., Gama, C., Chichorro, M., et al., 2016. Evidence for Multi-Cycle Sedimentation and Provenance Constraints from Detrital Zircon U-Pb Ages: Triassic Strata of the Lusitanian Basin (Western Iberia). *Tectonophysics*, 681: 318 – 331. <https://doi.org/10.1016/j.tecto.2015.10.011>
- Qi, K., Ren, Z. L., Cui, J. P., et al., 2017. The Meso-Cenozoic Tectonic Thermal Evolution of the Qishan-Linyou Areas in Weibei Uplift of Ordos Basin and Its Response in Geology: Evidence from Fission-Track Analysis. *Acta Geologica Sinica*, 91(1): 151 – 162 (in Chinese with English Abstract)
- Qiao, D. W., Kuang, H. W., Liu, Y. Q., et al., 2020. Identification of Eolian Sandstone in Cretaceous Uraniferous Sandstone in Ordos Basin, China. *Geotectonica et Metallogenia*, 44(4): 648–666 (in Chinese with English Abstract)
- Qin, H. P., Wu, C. L., Wu, X. P., et al., 2012. LA-ICP-MS Zircon U-Pb Ages and Implications for Tectonic Setting of the Mangling Granitoid Plutons in Qinling Orogen Belt. *Geological Review*, 58(4): 783–793 (in Chinese with English Abstract)
- Qin, Z. W., Wu, Y. B., Siebel, W., et al., 2015. Genesis of Adakitic Granitoids by Partial Melting of Thickened Lower Crust and Its Implications for Early Crustal Growth: A Case Study from the

- Huichizi Pluton, Qinling Orogen, Central China. *Lithos*, 238: 1–12. <https://doi.org/10.1016/j.lithos.2015.09.017>
- Ratschbacher, L., Hacker, B. R., Calvert, A., et al., 2003. Tectonics of the Qinling (Central China): Tectonostratigraphy, Geochronology, and Deformation History. *Tectonophysics*, 366(1/2): 1–53. [https://doi.org/10.1016/s0040-1951\(03\)00053-2](https://doi.org/10.1016/s0040-1951(03)00053-2)
- Ritts, B. D., Hanson, A. D., Darby, B. J., et al., 2004. Sedimentary Record of Triassic Intraplate Extension in North China: Evidence from the Nonmarine NW Ordos Basin, Helan Shan and Zhuozi Shan. *Tectonophysics*, 386(3/4): 177–202. <https://doi.org/10.1016/j.tecto.2004.06.003>
- Rogers, J. J. W., Santosh, M., 2009. Tectonics and Surface Effects of the Supercontinent Columbia. *Gondwana Research*, 15(3/4): 373–380. <https://doi.org/10.1016/j.gr.2008.06.008>
- Rong, H., Jiao, Y. Q., Wu, L. Q., et al., 2019. Origin of the Carbonaceous Debris and Its Implication for Mineralization within the Qianjiadian Uranium Deposit, Southern Songliao Basin. *Ore Geology Reviews*, 107: 336–352. <https://doi.org/10.1016/j.oregeorev.2019.02.036>
- Sanford, R. F., 1982. Preliminary Model of Regional Mesozoic Groundwater Flow and Uranium Deposition in the Colorado Plateau. *Geology*, 10(7): 348–352. [https://doi.org/10.1130/0091-7613\(1982\)10348:pmormg>2.0.co;2](https://doi.org/10.1130/0091-7613(1982)10348:pmormg>2.0.co;2)
- Shen, K. F., Yang, J. X., Hou, S. R., et al., 2014. Uranium Prospecting Breakthrough, Achievement Expanding and Prospecting Orientation in Main Mesozoic–Cenozoic Sedimentary Uranium Basins of Inner Mongolia. *Geology in China*, 41(4): 1304–1313 (in Chinese with English Abstract)
- Shi, R. D., Yang, J. S., Wu, C. L., et al., 2004. First SHRIMP Dating for the Formation of the Late Sinian Yushigou Ophiolite, North Qilian Mountains. *Acta Geologica Sinica*, 78(5): 649–657 (in Chinese with English Abstract)
- Shi, X. J., Zhang, L., Zhang, C. G., et al., 2020. Zircon Geochronology and Geochemistry of the Granitoids in Yagan Area, Northern Alxa and Their Tectonic Implications. *Earth Science*, 45(7): 2469–2484 (In Chinese with English Abstract)
- Shi, X. J., Tong, Y., Wang, T., et al., 2012. LA-ICP-MS Zircon U-Pb Age and Geochemistry of the Early Permian Halinudeng Granite in Northern Alxa Area, Western Inner Mongolia. *Geological Bulletin of China*, 31(5): 662–670 (in Chinese with English Abstract)
- Shi, X. J., Zhang, L., Wang, T., et al., 2016. Zircon Geochronology and Hf Isotopic Compositions for the Mesoproterozoic Gneisses in Zongnaishan Area, Northern Alxa and Its Tectonic Affinity. *Acta Petrologica Sinica*, 32(11): 3518–3536 (in Chinese with English Abstract)
- Shi, Y., Yu, J. H., Santosh, M., 2013. Tectonic Evolution of the Qinling Orogenic Belt, Central China: New Evidence from Geochemical, Zircon U-Pb Geochronology and Hf Isotopes. *Precambrian Research*, 231: 19–60. <https://doi.org/10.1016/j.precamres.2013.03.001>
- Söderlund, U., Patchett, P. J., Vervoort, J. D., et al., 2004. The ¹⁷⁶Lu Decay Constant Determined by Lu-Hf and U-Pb Isotope Systematics of Precambrian Mafic Intrusions. *Earth and Planetary Science Letters*, 219(3/4): 311–324. [https://doi.org/10.1016/S0012-821X\(04\)00012-3](https://doi.org/10.1016/S0012-821X(04)00012-3)
- Song, D. F., Xiao, W. J., Collins, A. S., et al., 2017. New Chronological Constrains on the Tectonic Affinity of the Alxa Block, NW China. *Precambrian Research*, 299: 230–243. <https://doi.org/10.1016/j.precamres.2017.07.015>
- Song, L. J., Chen, J. L., Zhang, Y. L., et al., 2010. U-Pb Chronological Characteristics of Late Triassic Sediment in Southwestern Ordos and Its Tectonic Significance. *Acta Geologica Sinica*, 84(3): 370–386 (in Chinese with English Abstract)
- Steffen, D., Schlunegger, F., Preusser, F., 2010. Late Pleistocene Fans and Terraces in the Majes Valley, Southern Peru, and Their Relation to Climatic Variations. *International Journal of Earth Sciences*, 99(8): 1975–1989. <https://doi.org/10.1007/s00531-009-0489-2>
- Su, Y. P., Zheng, J. P., Griffin, W. L., et al., 2014. Zircon U-Pb Ages and Hf Isotope of Gneissic Rocks from the Huai'an Complex: Implications for Crustal Accretion and Tectonic Evolution in the Northern Margin of the North China Craton. *Precambrian Research*, 255: 335–354. <https://doi.org/10.1016/j.precamres.2014.10.007>
- Sun, D., Feng, Q., Liu, Z., et al., 2017. Detrital Zircon U-Pb Dating of the Upper Triassic Yanchang Formation in Southwestern Ordos Basin and Its Provenance Significance. *Acta Geologica Sinica*, 91(11): 2521–2544 (in Chinese with English Abstract)
- Sun, L. X., Zhang, Y., Zhang, T. F., et al., 2017. Jurassic Sporopollen of Yan'an Formation and Zhiluo Formation in the North-Eastern Ordos Basin, Inner Mongolia, and Its Paleoclimatic Significance. *Earth Science Frontiers*, 24(1): 32–51 (in Chinese with English Abstract)
- Tao, G., Zhu, L. D., Li, Z. W., et al., 2017. Petrogenesis and Geological Significance of the North Liuhuangkuang Granodiorite in the West Sement of the Qilian Terrane: Evidences from Geochronology, Geochemistry, and Hf Isotopes. *Earth Science*, 42(12): 2258–2275 (in Chinese with English Abstract)
- Thomas, W. A., 2011. Detrital-Zircon Geochronology and Sedimentary Provenance. *Lithosphere*, 3(4): 304–308. <https://doi.org/10.1130/rf.1001.1>
- Trap, P., Faure, M., Lin, W., et al., 2007. Late Paleoproterozoic (1 900–1 800 Ma) Nappe Stacking and Polyphase Deformation in the Hengshan-Wutaishan Area: Implications for the Understanding of the Trans-North-China Belt, North China Craton. *Precambrian Research*, 156(1/2): 85–106. <https://doi.org/10.1016/j.precamres.2007.03.001>
- Tseng, C. Y., Yang, H. J., Yang, H. Y., et al., 2007. The Dongcaohe Ophiolite from the North Qilian Mountains: A Fossil Oceanic Crust of the Paleo-Qilian Ocean. *Chinese Science Bulletin*, 52(17): 2390–2401. <https://doi.org/10.1007/s11434-007-0300-3>
- Wan, Y. S., Liu, D. Y., Wang, W., et al., 2011. Provenance of Meso- to Neoproterozoic Cover Sediments at the Ming Tombs, Beijing, North China Craton: An Integrated Study of U-Pb Dating and Hf Isotopic Measurement of Detrital Zircons and Whole-Rock Geochemistry. *Gondwana Research*, 20(1): 219–242. <https://doi.org/10.1016/j.gr.2011.02.009>
- Wang, F., Chen, F. K., Hou, Z. H., et al., 2009. Zircon Ages and Sr-Nd-Hf Isotopic Composition of Late Paleozoic Granitoids in the Chongli-Chicheng Area, Northern Margin of the North China Block. *Acta Petrologica Sinica*, 25(11): 3057–3074 (in Chinese with English Abstract)
- Wang, H., Wu, Y. B., Gao, S., et al., 2013. Continental Origin of Eclogites in the North Qinling Terrane and Its Tectonic Implications. *Precambrian Research*, 230: 13–30. <https://doi.org/10.1016/j.precamres.2012.12.010>
- Wang, J. Q., 2010. Mesozoic-Cenozoic Basin Evolution-Reforming and Basin-Mountain Coupling in Southern Ordos Basin: [Dissertation]. Northwest University, Xi'an (in Chinese with English Abstract)
- Wang, J. X., Nie, F. J., Zhang, X. N., et al., 2016. Molybdenite Re-Os, Zircon U-Pb Dating and Lu-Hf Isotopic Analysis of the Xiaerchulu Au Deposit, Inner Mongolia Province, China. *Lithos*, 261: 356–372. <https://doi.org/10.1016/j.lithos.2016.06.008>
- Wang, L., Wang, G. H., Lei, S. B., et al., 2015. Petrogenesis of Dahuabei

- Pluton from Wulashan, Inner Mongolia: Constraints from Geochemistry, Zircon U-Pb Dating and Sr-Nd-Hf Isotopes. *Acta Petrologica Sinica*, 31(7): 1977 – 1994 (in Chinese with English Abstract)
- Wang, M., Luo, J. L., Li, M., et al., 2013. Provenance and Tectonic Setting of Sandstone-Type Uranium Deposit in Dongsheng Area, Ordos Basin: Evidence from U-Pb Age and Hf Isotopes of Detrital Zircons. *Acta Petrologica Sinica*, 29(8): 2746 – 2758 (in Chinese with English Abstract)
- Wang, S. B., Yang, J., Li, J. G., et al., 2018. Elemental Geochemical Characteristics of Jurassic Uranium-Bearing Strata in Ningdong Area, Western Ordos Basin. *Coal Geology & Exploration*, 46(6): 19–25, 32 (in Chinese with English Abstract)
- Wang, T., Wang, X. X., Tian, W., et al., 2009. North Qinling Paleozoic Granite Associations and Their Variation in Space and Time: Implications for Orogenic Processes in the Orogens of Central China. *Science in China, Series D (Earth Sciences)*, 39(7): 949 – 971 (in Chinese with English Abstract)
- Wang, X. X., Wang, T., Jahn, B. M., et al., 2007. Tectonic Significance of Late Triassic Post-Collisional Lamprophyre Dykes from the Qinling Mountains (China). *Geological Magazine*, 144(5): 837–848. <https://doi.org/10.1017/s0016756807003548>
- Wang, X. X., Wang, T., Qi, Q. J., et al., 2011b. Temporal-Spatial Variations, Origin and Their Tectonic Significance of the Late Mesozoic Granites in the Qinling, Central China. *Acta Petrologica Sinica*, 27(6): 1573–1593 (in Chinese with English Abstract)
- Wang, X. X., Wang, T., Zhang, C. L., 2015. Granitoid Magmatism in the Qinling Orogen, Central China and Its Bearing on Orogenic Evolution. *Science China Earth Sciences*, 58(9): 1497 – 1512. <https://doi.org/10.1007/s11430-015-5150-2>
- Wang, X., Williams, L. G., Chen, J., et al., 2011a. U and Th Contents and U/Th Ratios of Zircon in Felsic and Mafic Magmatic Rocks: Improved Zircon-Melt Distribution Coefficients. *Acta Geologica Sinica*, 85(1): 164–174. <https://doi.org/10.1111/j.1755-6724.2011.00387.x>
- Wang, Y. C., Pei, X. Z., Li, Z. C., et al., 2012. LA-ICP-MS Zircon U-Pb Dating of the Mesoproterozoic Granitic Gneisses at Changningyi of Zhangjiachuan Area on the Eastern Edge of the Qilian Orogenic Belt. *Geological Bulletin of China*, 31(10): 1576 – 1587 (in Chinese with English Abstract)
- Wang, Z. Z., Han, B. F., Feng, L. X., et al., 2015. Geochronology, Geochemistry and Origins of the Paleozoic-Triassic Plutons in the Langshan Area, Western Inner Mongolia, China. *Journal of Asian Earth Sciences*, 97: 337–351. <https://doi.org/10.1016/j.jseas.2014.08.005>
- Wei, B., Zhang, Z. Y., Yang, Y. Y., 2006. Sedimentary Facies of the Cretaceous Luohe and Huanhe-Huachi Formations in the Ordos Basin. *Journal of Stratigraphy*, 30(4): 367 – 372 (in Chinese with English Abstract)
- Windley, B. F., Alexeiev, D., Xiao, W. J., et al., 2007. Tectonic Models for Accretion of the Central Asian Orogenic Belt. *Journal of the Geological Society*, 164(1): 31 – 47. <https://doi.org/10.1144/0016-76492006-022>
- Wu, C. L., Xu, X. Y., Gao, Q. M., et al., 2010. Early Palaeozoic Granitoid Magmatism and Tectonic Evolution in North Qilian, NW China. *Acta Petrologica Sinica*, 26(4): 1027 – 1044 (in Chinese with English Abstract)
- Wu, F. Y., Li, X. H., Zheng, Y. F., et al., 2007. Lu-Hf Isotopic Systematics and Their Applications in Petrology. *Acta Petrologica Sinica*, 23(2): 185 – 220 (in Chinese with English Abstract)
- Wu, F. Y., Yang, Y. H., Xie, L. W., et al., 2006. Hf Isotopic Compositions of the Standard Zircons and Baddeleyites Used in U-Pb Geochronology. *Chemical Geology*, 234(1/2): 105 – 126. <https://doi.org/10.1016/j.chemgeo.2006.05.003>
- Wu, Y. B., Zheng, Y. F., 2004. Genesis of Zircon and Its Constraints on Interpretation of U-Pb Age. *Chinese Science Bulletin*, 49(15): 1554–1569. <https://doi.org/10.1007/bf03184122>
- Xia, L. Q., Li, X. M., Yu, J. Y., et al., 2016. Mid-Late Neoproterozoic to Early Paleozoic Volcanism and Tectonic Evolution of the Qilian Mountain. *Geology in China*, 43(4): 1087 – 1138 (in Chinese with English Abstract)
- Xiao, W. J., Santosh, M., 2014. The Western Central Asian Orogenic Belt: A Window to Accretionary Orogenesis and Continental Growth. *Gondwana Research*, 25(4): 1429 – 1444. <https://doi.org/10.1016/j.gr.2014.01.008>
- Xie, F. Q., Sun, Y. H., Wang, L. D., et al., 2020. Petrogenesis and Tectonic Setting of the Chaheilingashun Pluton, North Alxa Block, NW China: Constraints from Whole-Rock Geochemistry, Zircon U-Pb Ages, and Hf Isotope Compositions. *Arabian Journal of Geosciences*, 13(14): 1–13. <https://doi.org/10.1007/s12517-020-05658-3>
- Xie, H. L., Jiao, Y. Q., Liu, Z. Y., et al., 2020. Occurrence and Enrichment Mechanism of Uranium Ore Minerals from Sandstone-Type Uranium Deposit, Northern Ordos Basin. *Earth Science*, 45(5): 1531–1543 (in Chinese with English Abstract)
- Xie, L. W., Zhang, Y. B., Zhang, H. H., et al., 2008. *In situ* Simultaneous Determination of Trace Elements, U-Pb and Lu-Hf Isotopes in Zircon and Baddeleyite. *Chinese Science Bulletin*, 53(10): 1565–1573. <https://doi.org/10.1007/s11434-008-0086-y>
- Xie, X. Y., Heller, P. L., 2013. U-Pb Detrital Zircon Geochronology and Its Implications: The Early Late Triassic Yanchang Formation, South Ordos Basin, China. *Journal of Asian Earth Sciences*, 64: 86–98. <https://doi.org/10.1016/j.jseas.2012.11.045>
- Xing, X. W., Wang, Y. J., Zhang, Y. Z., 2016. Detrital Zircon U-Pb Geochronology and Lu-Hf Isotopic Compositions of the Wuliangshan Metasediment Rocks in SW Yunnan (China) and Its Provenance Implications. *Journal of Earth Science*, 27(3): 412–424. <https://doi.org/10.1007/s12583-015-0647-3>
- Xu, B., Xiao, S. H., Zou, H. B., et al., 2009. SHRIMP Zircon U-Pb Age Constraints on Neoproterozoic Quruqtagh Diamictites in NW China. *Precambrian Research*, 168(3/4): 247–258. <https://doi.org/10.1016/j.precamres.2008.10.008>
- Xu, X. Y., Wang, H. L., Chen, J. L., et al., 2008. Zircon U-Pb Dating and Petrogenesis of Xinglongshan Group Basic Volcanic Rocks at Eastern Segment of Middle Qilian Mts. *Acta Petrologica Sinica*, 24(4): 827–840 (in Chinese with English Abstract)
- Xu, Y. J., Du, Y. S., Cawood, P. A., et al., 2010. Detrital Zircon Record of Continental Collision: Assembly of the Qilian Orogen, China. *Sedimentary Geology*, 230(1/2): 35 – 45. <https://doi.org/10.1016/j.sedgeo.2010.06.020>
- Xue, C. J., Chi, G. X., Xue, W., 2010. Interaction of Two Fluid Systems in the Formation of Sandstone-Hosted Uranium Deposits in the Ordos Basin: Geochemical Evidence and Hydrodynamic Modeling. *Journal of Geochemical Exploration*, 106(1/2/3): 226 – 235. <https://doi.org/10.1016/j.jgexplo.2009.11.006>
- Yang, F., Chen, G., Chen, Q., et al., 2015. U-Pb Dating of Detrital Zircon from Upper Ordovician Pingliang Formation in Southwest Margin of the Ordos Basin and Provenance Analysis. *Geological Review*, 61(1): 172–182 (in Chinese with English Abstract)

- Yang, H., Zhang, H. F., Luo, B. J., et al., 2015. Early Paleozoic Intrusive Rocks from the Eastern Qilian Orogen, NE Tibetan Plateau: Petrogenesis and Tectonic Significance. *Lithos*, 224/225: 13–31. <https://doi.org/10.1016/j.lithos.2015.02.020>
- Yang, L., Chen, F. K., Yang, Y. Z., et al., 2010. Zircon U-Pb Ages of the Qinling Group in Danfeng Area: Recording Mesoproterozoic and Neoproterozoic Magmatism and Early Paleozoic Metamorphism in the North Qinling Terrain. *Acta Petrologica Sinica*, 26(5): 1589–1603 (in Chinese with English Abstract)
- Yang, X. Y., Ling, M. X., Sun, W. D., et al., 2009. The Genesis of Sandstone-Type Uranium Deposits in the Ordos Basin, NW China: Constraints Provided by Fluid Inclusions and Stable Isotopes. *International Geology Review*, 51(5): 422–455. <https://doi.org/10.1080/00206810902757339>
- Yang, Y., Wang, X. X., Ke, C. H., et al., 2014. Zircon U-Pb Ages, Geochemistry and Evolution of Mangling Pluton in North Qinling Mountains. *Mineral Deposits*, 33(1): 14–36 (in Chinese with English Abstract)
- Yang, Z., Dong, Y. P., Liu, X. M., et al., 2006b. LA-ICP-MS Zircon U-Pb Dating of Gabbro in the Guanzizhen Ophiolite, Tianshui, West Qinling, China. *Geological Bulletin of China*, 25(11): 1321–1325 (in Chinese with English Abstract)
- Yi, Z. Y., Liu, Y. Q., Meert, J. G., 2019. A True Polar Wander Trigger for the Great Jurassic East Asian Aridification. *Geology*, 47(12): 1112–1116. <https://doi.org/10.1130/g46641.1>
- Yu, R. A., Si, Q. H., Wang, S. B., et al., 2020. Geochemical Characteristics and Detrital Zircon U-Pb Ages of the Zhiluo Formation in the Shicaocun Area of the Western Ordos Basin and Implication for its Tectonic Setting and Provenance. *Geotectonica et Metallogenia*, 44(4): 754–771 (in Chinese with English abstract)
- Yuan, H. L., Gao, S., Dai, M. N., et al., 2008. Simultaneous Determinations of U-Pb Age, Hf Isotopes and Trace Element Compositions of Zircon by Excimer Laser-Ablation Quadrupole and Multiple-Collector ICP-MS. *Chemical Geology*, 247(1/2): 100–118. <https://doi.org/10.1016/j.chemgeo.2007.10.003>
- Zeng, L. J., Xing, Y. C., Zhou, D., et al., 2013. LA-ICP-MS Zircon U-Pb Age and Hf Isotope Composition of the Babaoshan Granite Porphyries in Lushi County, Henan Province. *Geotectonica et Metallogenia*, 37(1): 65–77 (in Chinese with English Abstract)
- Zhai, M. G., 2011. Cratonization and the Ancient North China Continent: A Summary and Review. *Science China Earth Sciences*, 54(8): 1110–1120. <https://doi.org/10.1007/s11430-011-4250-x>
- Zhai, M. G., Santosh, M., 2011. The Early Precambrian Odyssey of the North China Craton: A Synoptic Overview. *Gondwana Research*, 20(1): 6–25. <https://doi.org/10.1016/j.gr.2011.02.005>
- Zhai, M. G., Peng, P., 2007. Paleoproterozoic Events in the North China Craton. *Acta Petrologica Sinica*, 23(11): 2665–2682 (in Chinese with English Abstract)
- Zhang, C. L., Liu, L., Wang, T., et al., 2013. Granitic Magmatism Related to Early Paleozoic Continental Collision in North Qinling. *Chinese Science Bulletin*, 58(35): 4405–4410. <https://doi.org/10.1007/s11434-013-6064-z>
- Zhang, H., Jin, X. L., Li, G. H., et al., 2008. Original Features and Palaeogeographic Evolution during the Jurassic–Cretaceous in Ordos Basin. *Journal of Palaeogeography*, 10(1): 1–11 (in Chinese with English Abstract)
- Zhang, J., Li, J. Y., Liu, J. F., et al., 2012. The Relationship between the Alxa Block and the North China Plate during the Early Paleozoic: New Information from the Middle Ordovician Detrital Zircon Ages in the Eastern Alxa Block. *Acta Petrologica Sinica*, 28(9): 2912–2934 (in Chinese with English Abstract)
- Zhang, J., Zhang, B. H., Zhao, H., 2016. Timing of Amalgamation of the Alxa Block and the North China Block: Constraints Based on Detrital Zircon U-Pb Ages and Sedimentologic and Structural Evidence. *Tectonophysics*, 668/669: 65–81. <https://doi.org/10.1016/j.tecto.2015.12.006>
- Zhang, J. J., Zhang, L., Wang, T., et al., 2019. Geochemical, Age and Hf-in-Zircon Isotopic Characteristics and Geological Significance of Granite and MME from the Mandelinwula Pluton, Northern Alxa Block, Inner Mongolia. *Geological Bulletin of China*, 38(10): 1675–1690 (in Chinese with English Abstract)
- Zhang, J. X., Xu, Z. Q., Chen, W., et al., 1997. A Tentative Discussion on the Ages of the Subduction-Accretionary Complex/Volcanic Arcs in the Middle Sector of North Qilian Mountain. *Acta Petrologica et Mineralogica*, 16(2): 112–119 (in Chinese with English Abstract)
- Zhang, J. Y., He, Y. H., Chen, L., et al., 2019. Paleozoic Magma Evolution at the Eastern End of Northern Qilian Orogenic Belt: Evidence from the Zircon U-Pb Ages, Trace Elements and Hf Isotopic Composition of Changgouhe Dioritic Gneiss. *Geological Bulletin of China*, 38(10): 1626–1636 (in Chinese with English Abstract)
- Zhang, L. Q., Zhang, H. F., Zhang, S. S., et al., 2017. Lithospheric Delamination in Post-Collisional Setting: Evidence from Intrusive Magmatism from the North Qilian Orogen to Southern Margin of the Alxa Block, NW China. *Lithos*, 288/289: 20–34. <https://doi.org/10.1016/j.lithos.2017.07.009>
- Zhang, P. Z., Molnar, P., Downs, W. R., 2001. Increased Sedimentation Rates and Grain Sizes 2–4 Myr Ago due to the Influence of Climate Change on Erosion Rates. *Nature*, 410(6831): 891–897. <https://doi.org/10.1038/35073504>
- Zhang, Q., Li, Y. H., Chen, G. C., et al., 2018. Geochronology, Geochemistry, and Hf Isotopic Compositions of the Late-Carboniferous Volcanic Rocks in Tongshengmao of Daqinshan Area, Inner Mongolia and Their Geological Implications. *Geological Journal of China Universities*, 24(2): 160–171 (in Chinese with English Abstract)
- Zhang, S. H., Zhao, Y., Song, B., et al., 2006. Contrasting Late Carboniferous and Late Permian–Middle Triassic Intrusive Suites from the Northern Margin of the North China Craton: Geochronology, Petrogenesis, and Tectonic Implications. *Geological Society of America Bulletin*, 121(1/2): 181–200. <https://doi.org/10.1130/b26157.1>
- Zhang, X., Nie, F. J., Xia, F., et al., 2018. Provenance Constraints on the Xishanyao Formation, Southern Yili Basin, Northwest China: Evidence from Petrology, Geochemistry, and Detrital Zircon U-Pb Geochronology. *Canadian Journal of Earth Sciences*, 55(9): 1020–1035. <https://doi.org/10.1139/cjes-2017-0258>
- Zhang, Y. P., Chen, X. H., Zhang, J., 2016. Geochronology and Tectonic Implications of Diabase Intruded into Xiangshan Group in the Southeastern Alxa Block, NW China. *Acta Geologica Sinica—English Edition*, 90(s1): 88–91. <https://doi.org/10.1111/1755-6724.12904>
- Zhang, Z. L., Fan, H. H., He, F., et al., 2018. Analysis of Sandstone Type Uranium Metallogenic Conditions of Lower Cretaceous in the Southwest Margin of Ordos Basin. *Uranium Geology*, 34(4): 193–200 (in Chinese with English Abstract)
- Zhao, C. Y., Jin, J. Q., 2011. *Geology of Petroliferous Basins*. Petroleum Industry Press, Beijing (in Chinese)
- Zhao, H. L., Li, J. G., Miao, P. S., et al., 2020. Mineralogical Study of Pengyang Uranium Deposit and Its Significance of Regional Mineral

- Exploration in Southwestern Ordos Basin. *Geotectonica et Metallogenia*, 44(4): 607–618 (in Chinese with English Abstract)
- Zhao, J. F., Liu, C. Y., Huang, L., et al., 2020. Paleogeography Reconstruction of a Multi-Stage Modified Intra-Cratonic Basin—A Case Study from the Jurassic Ordos Basin, Western North China Craton. *Journal of Asian Earth Sciences*, 190: 104191. <https://doi.org/10.1016/j.jseaes.2019.104191>
- Zhao, J. F., Liu, C. Y., Liang, J. W., et al., 2010. Restoration of the Original Sedimentary Boundary of the Middle Jurassic Zhiluo Formation—Anding Formation in the Ordos Basin. *Acta Geologica Sinica*, 84(4): 553–569 (in Chinese with English Abstract)
- Zhao, J. F., Liu, C. Y., Wang, X. M., et al., 2009. Migration of Depocenters and Accumulation Centers and Its Indication of Subsidence Centers in the Mesozoic Ordos Basin. *Acta Geologica Sinica*, 83(2): 278–294 (in Chinese with English Abstract)
- Zhao, X. C., Liu, C. Y., Wang, J. Q., et al., 2020. Provenance Analyses of Lower Cretaceous Strata in the Liupanshan Basin: From Paleocurrents Indicators, Conglomerate Clast Compositions, and Zircon U-Pb Geochronology. *Journal of Earth Science*, 31(4): 757–771. <https://doi.org/10.1007/s12583-020-1324-8>
- Zheng, R. G., Zhang, J., Xiao, W. J., 2019. Association of Permian Gabbro and Granite in the Langshan, Southern Central Asian Orogenic Belt: Age, Origin, and Tectonic Implications. *Lithos*, 348/349: 105174. <https://doi.org/10.1016/j.lithos.2019.105174>
- Zheng, Y. F., Xiao, W. J., Zhao, G. C., 2013. Introduction to Tectonics of China. *Gondwana Research*, 23(4): 1189 – 1206. <https://doi.org/10.1016/j.gr.2012.10.001>
- Zhou, H., Zhao, G. C., Han, Y. G., et al., 2018. Geochemistry and Zircon U-Pb-Hf Isotopes of Paleozoic Intrusive Rocks in the Damao Area in Inner Mongolia, Northern China: Implications for the Tectonic Evolution of the Bainaimiao Arc. *Lithos*, 314/315: 119–139. <https://doi.org/10.1016/j.lithos.2018.05.020>
- Zhou, L. R., Yu, P. S., 1989. Isotopic Age of Alxa Platform and Its Geological Significance. *Northwestern Geology*, 6: 52–63 (in Chinese with English Abstract)
- Zhou, W. Y., Jiao, Y. Q., Zhao, J. H., 2017. Sediment Provenance of the Intracontinental Ordos Basin in North China Craton Controlled by Tectonic Evolution of the Basin-Orogen System. *The Journal of Geology*, 125(6): 701–711. <https://doi.org/10.1086/693861>
- Zhu, Q., Li, J. G., Miao, P. S., et al., 2019. Reservoir Characteristics of Luohe Formation and Metallogenic Geological Conditions of Deep Uranium in the Southwestern Margin of Ordos Basin, China. *Journal of Earth Sciences and Environment*, 41(6): 675–690 (in Chinese with English Abstract)
- Zhu, X. R., Liu, L., Jia, S. J., et al., 2018. Geochemical and Provenance Characteristics of Eolian Sandstone of Cretaceous Luohe Formation in Ordos Basins: An Example from Outcrop in Longzhou, Jingbian. *Global Geology*, 37(3): 702–711 (in Chinese with English Abstract)